Assessing Irrigation Influences on Hydrological Components in Endorheic Basins including Climate Change Consideration

Doctoral Thesis

Thesis Title

Assessing irrigation influences on hydrological components in endorheic basins including climate change consideration

(気候変動を考慮した内陸湖流域の水文環境に対する灌漑の影響評価)

Department of Civil and Environmental Engineering

Graduate school of Engineering,

TOHOKU UNIVERSITY

JACQUELINE MUTHONI MBUGUA

Advising Professor at Tohoku Univ.	Professor So Kazama
Research Advisor at Tohoku Univ.	Assistant Professor Yoshiya Touge
Dissertation Committee Members Name marked with "○" is the Chief Examiner	○ Professor So Kazama 1 Professor Hitoshi Tanaka　2 Associate Professor Daisuke Komori 3 Associate Professor Eric Mas　4 5　6

ACKNOWLEDGMENT

All glory and honor to the Almighty God for his grace, eternal blessings, and benevolence; without him, all this would have been inconceivable.

Secondly, I would like to express my heartfelt appreciation to my thesis advisors, Professor So Kazama and Assistant Professor Yoshiya Touge of the Graduate School of Engineering. This doctoral dissertation has come to fruition through your insight, patience, endless support, and invaluable input to my work. Additionally, I would like to thank Professor Hitoshi Tanaka, Associate Professor Daisuke Komori, Associate Professor Makoto Umeda, Associate Professor Erick Mas, and Assistant Professor Nguyen Xuan Tinh. Your contribution has facilitated my growth as a researcher and encouraged me to set higher goals for myself.

I owe a debt of gratitude to the late Professor John f. Obiri. Part of this study was made possible thanks to his technical assistance. In addition, I am grateful to my fellow students for their contributions, cooperation, and friendship, especially Dr.Grace Puyang, who has been a reliable friend and colleague providing words of wisdom and encouragement throughout my 5-year study. Furthermore, I'm sincerely thankful to Dr.Anne Mutahi for her moral support and words of advice whenever I needed a confidence boost. Finally, I appreciate Chiaki Kakubari, who was always willing to assist throughout my years at the HEST lab.

My sincere gratitude to Japan's Ministry of Education, Culture, Sports, Science, and Technology for bestowing the Monbukagakusho Scholarship upon me (160779). I would also like to acknowledge Grant-in-Aid for Scientific Research (B), 2017-2022 (17H04585, Yoshiya Touge) from the Ministry of Education, Science, Sports, and Culture, which made this research possible.

Finally, I must express my heartfelt gratitude to my parents (Sammy and Teresa) and siblings (Millicent, Dennis, and Doris) for their unwavering support and encouragement throughout my years of study and the process of researching and writing this Manuscript. This accomplishment would not have been possible without their backing.

ASSESSING IRRIGATION INFLUENCES ON HYDROLOGICAL COMPONENTS IN ENDORHEIC BASINS INCLUDING CLIMATE CHANGE CONSIDERATION

ABSTRACT: Due to alterations in global endorheic basins, the water and heat balance cycles have recently changed. This is propagated by increased anthropogenic activities exacerbated by the climate. The most common anthropogenic-induced alteration is the expansion of irrigated areas. The impacts of on the environment and potential disaster exposures are significant and widespread. Thus, understanding what factors affect water circulation in a basin and the environmental consequences is scientifically imperative. Consequently, the principal concept for this study was to develop methodologies to estimate the sustainability of global endorheic Lakes, considering the irrigation-induced changes and climatic influences. In this study, literature review, remote sensing, and numerical simulation approaches were utilized. The Aral Sea Basin, known worldwide for its large expanse of irrigated area and effects instigated by it, and the Lake Turkana Basin, which is currently changing, are the focal study areas. The transformations in the Aral Sea Basin in Central Asia are one of the most egregious examples of environmental disasters facilitated by anthropogenic influences. Additionally, Lake Turkana is currently categorized as an endangered lake due to the ongoing activities in the basin that could threaten the lake's sustainability.

First, in order to understand the consequences instigated by changes in the terrestrial water circulation, changes in the Aral Sea basin were assessed. Historical changes reveal an inverse relationship between increasing irrigated area and decreasing sea area. For example, between 1960 and 1970, there was a 13 percent increase in irrigated areas, which resulted in a 10 percent drop in the sea level. A similar inverse relationship was described between increasing salinity and decreasing fishing stocks. The fishing industry was utterly destroyed when the salinity levels in the sea reached approximately 22 grams per liter. Moreover, a drop in the sea level was also linked to increasing disease incidents in this basin. When the Sea area had shrunk by nearly half, it was reported that almost 60 percent of children under the age of one who died in the Karakalpakstan region died of respiratory diseases.

Due to the expansive nature of irrigation activities in the Aral Sea basin, environmental problems such as increased soil salinization have become more prominent. Because of this, the actual irrigated area in the basin is constantly changing. Therefore, it is challenging to know the exact area under irrigation, and the existing irrigation area datasets fail to identify this land, especially during drought years. Thus, in this study, indices based on the Land Surface Model and Satellite Land Surface Temperature were developed to determine the actual irrigated area based on the heat capacity difference in soil with high moisture content. As a result, these indices could perceive the irrigation effect even in drought years. Furthermore, a sum of each index compared to water availability provided by dam data showed a similar trend, indicating the indices' ability to capture changes in the irrigated area. Remote sensing for salinity detection in the Aral Sea basin indicated the limitation instigated by the coarse Terra satellite resolution. No significant correlation was established between the indices employed to detect salinity gradation. However, the reflectance-based indices generally exhibited an increasing trend with an increase in salinity, while the vegetation indices decreased with an increase in salinity.

Then, since the Lake Turkana basin is currently changing, numerical simulation using the Simple Biosphere including Urban Canopy (SiBUC), was coupled with a developed lake water balance model to analyze changes in the basin-scale water circulation. This model could replicate trends in the Lake's changing water balance from 2001 to 2018 with a relatively strong correlation r of 0.82. Thus, the changing climate, particularly precipitation, was established to be the main driver for storage changes in this basin.

Finally, to assess the sustainability of endorheic lakes, the comparison of long-term volume and area trend variations was evaluated considering lakes with different degrees of alteration on their water balance. For this, future changes to the Lake Turkana water balance were projected for the end of the century, assuming three irrigation scenarios using the Global Circulation Model (GCM) BCC-CSM2-MR SSP585. The volume and area variations in the Aral Sea were compared to the current and future changes in Lake Turkana. Examining the variation of both volume and area in an endorheic lake can provide insight into the lake's sustainability level. The larger the changes in the trend and variation of volume and area, the more significant the impact of changes in water balance on the surrounding environment. Furthermore, examining changes in both area and volume variation can provide insight into the magnitude of short-term changes in the lake.

The outcomes of this research highlight the value and limitations of using satellite remote sensing and numerical analysis for the detection of instigated changes in the basin. Therefore, the conclusions inferred here can provide a body of expedient knowledge and a tool to facilitate the understanding of changes occurring in this basin to prevent and mitigate damages in endorheic basins.

TABLE OF CONTENTS

LIST OF ABBREVIATIONS

USGS	United States Geological Survey
GLCC	Global Land Cover Classification
ESA	European Space Agency
NDVI	Normalized Difference Vegetation Index
FAO	Food and Agricultural Organization
LST	Land Surface Temperature
MODIS	Moderate Resolution Imaging Spectroradiometer
UTC	Coordinated Universal Time
ICARDA	International Center for Agricultural Research in the Dry Areas
ICBA	International Center for Biosaline Agriculture
TDR	Time domain reflectometry
NDWI	Normalized Difference Water Index
DOY	Day of Year
SiBUC	Simple Biosphere including Urban Canopy

LIST OF FIGURES

LIST OF TABLES

Chapter 1

1 Introduction

1.1 Background

Endorheic basins give rise to endorheic lakes, which are closed terrestrial water bodies with no outflow. They are characteristically found in arid and semi-arid regions and are vulnerable to climatic and catchment changes. Due to the closed nature of these basins, their geographic location, and the increasing anthropogenic activities exacerbated by climate change, the water and heat balance cycles in these basins are being altered globally (Bai et al., 2011; Olaka et al., 2010). One of the most significant anthropogenic factors is the expansion of irrigation areas. Admittedly, agriculture is the world's largest consumer of freshwater, owing to this (Shiklomanov, 2000). It accounts for 70 percent of the total water withdrawal from rivers, lakes, and groundwater aquifers (Gleick, 2000; Water FAO, 2009). This figure may reach up to 90 percent in some developing countries (UNESCO, 2012). Ordinarily, irrigation is a necessary prerequisite for crop growth in arid areas. It is used to supplement rainfall and increase crop production.

Another factor that may increase water demand in the global endorheic basins is the preference for irrigated cropland, which has been shown to yield significantly more than rain-fed cropland (Dowgert, 2010; Li and Troy, 2018; Zheng et al., 2019). In some developing countries, irrigation is crucial for the production of cereals (Mottaleb et al., 2019; Pingali, P. L. & Heisey, 1999). It accounts for 59 percent of total cereal production, despite being grown on just 38 percent of all cereal allocated land in some developing countries (Rosegrant et al., 2002). Nevertheless, water demand is expected to worsen as a 14 percent increase is expected by 2030 (Bruinsma, 2017). Furthermore, population growth would contribute to increased

water exigence. Over the last 100 years, global freshwater demand has risen by nearly 600 percent (Wada et al., 2016). Owing to several factors, including increased population, economic growth, and changing consumer patterns, water demand has been rising at a rate of 1 percent per year for the past decade. (Boretti and Rosa, 2019; Ringler, 2012; UNESCO, 2018).

Additionally, the demand for freshwater will rise in Africa and Asia's developing and emerging economies, where population growth is projected to be higher. (UNESCO, 2012; United Nations, 2017). As a result, the anthropogenic impacts in global endorheic basins are expected to intensify over time, altering the heat and water balance cycles in these basins. Climate change is also a significant source of worldwide endorheic basins' heat and water balance cycle shifts. The rise in temperature due to drought stress is one way this is having an impact (IPCC, 2014). If this happens, the need for irrigation water to improve crop productivity will be required, further exacerbating the problem.

One of the most egregious examples of environmental disasters facilitated by anthropogenic influences is the transformations in the Aral Sea Basin in Central Asia. From the late nineteenth century until the fall of the Soviet Union in 1991, the Soviet Socialist Republics (USSR) developed a large-scale irrigation project in the region, which rapidly expanded (Glantz, 1999; Micklin, 2000). Following this, the two major rivers that flow into the Aral Sea, the Amu Darya and the Syr Darya, experienced decreased flow into their deltas. Chiefly, as a result of more water abstraction for irrigation purposes. The volume of water reaching the Sea decreased dramatically, resulting in its shrinkage. Currently, the Sea's surface area is roughly 10 percent of its original size (Micklin and Aladin, 2008).

Lake Chad's desiccation in west-central Africa is a case in point of climate change impact on endorheic lakes. Precipitation in the region declined significantly over the last four decades,

resulting in drought conditions. As a result, uncapped boreholes were drilled, and a large-scale irrigation scheme was established. Consequently, this had a considerable impact on the drainage of the lakes basin. Subsequently, the Lake became desiccated (Birkett, 2000; Guganesharajah and Shaw, 1984). Although the changes in the Lake basins mentioned above resulted in the Lake shrinking, changes in water and heat balance cycles in a basin can also have the opposite effect. For example, owing to the Caspian Sea's dramatic fluctuation during the twentieth century, flooding was severe when the water level increased, and fisheries and marine transportation were harmed when the water level decreased. The explanation, however, remains obscure (Rodionov, 2012). The phenomena of extreme water fluctuations are significant in endorheic lakes worldwide. Changes in basin-scale water balance easily affect the water level and area of these lakes monthly and annually due to the small ratio of water volume storage to annual inflow in an endorheic lake.

These examples demonstrate that continental inland lakes are sensitive to changes in terrestrial water circulation. Furthermore, the effects of these changes on the environment and impending disaster exposures are considerable and widespread. Therefore, understanding what factors affect water circulation in a basin, and the resultant consequences for the environment are scientifically imperative. This body of knowledge is also socially expedient as information for preventing and mitigating damages in endorheic basins. It's challenging to replicate variations in a lake's water balance in the face of climate change and anthropogenic influences. However, since this study is based on a basin-scale approach for water balance consideration, any climatic and anthropogenic impacts in the basin can be evaluated through their influence on the Lake's resulting influx.

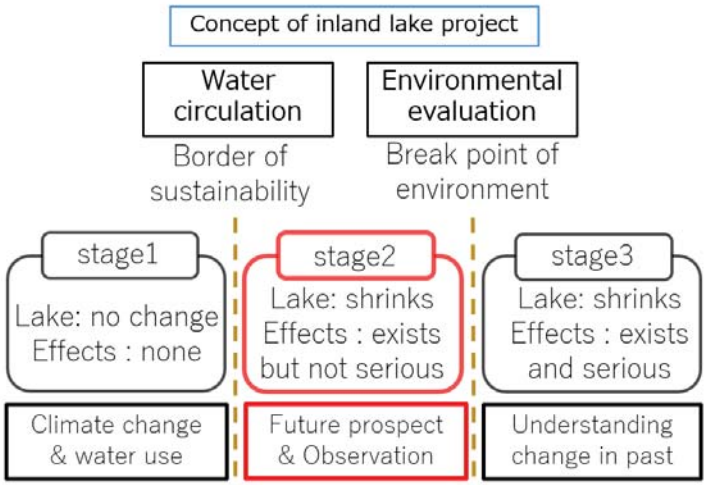

Fig. 1.1-1 Concept of the global inland lake project

The study's principal concept was developed based on three types of endorheic lakes (See Fig. 1.1-1 pg.4); (i) Stable lakes with no long-term changes in water storage, (ii) Lakes in danger of shrinking due to increasing anthropogenic influences in the basin, which are exacerbated by climate change, and (iii) Severely desiccated Lakes. This study aims to develop methodologies to consider the sustainability of lakes in (ii) above.

The main focus of this research is the Aral Sea in Central Asia and Lake Turkana in Eastern Africa. These water bodies are found in endorheic basins located in arid and semi-arid environments. Since the Aral Sea is already severely depleted, it is considered a changed endorheic lake in category (iii) in this research. On the other hand, Lake Turkana is regarded as a changing lake in category (ii) due to increased anthropogenic activities in the basin, which may jeopardize the Lake's existence.

1.2 Aims and Objectives

As a result, this research aims to develop methodologies to assess irrigation influences on hydrological components in endorheic basins, taking climate change into account, per the five objectives listed below:

1. To identify changes occurring in endorheic basins by comparing Lake Turkana to the Aral Sea.
2. To improve the detection of irrigation areas in arid regions by developing LST-based indices derived from satellite and a land surface model.
3. To elucidate the capability of remote sensing in detecting soil salinity in endorheic basins.
4. To explain changes in the water balance of endorheic lakes by developing a storage change model integrated with a land surface model.
5. To assess sustainability in endorheic lakes by considering long-term water balance changes in lakes of different status.

1.3 Outline of the Dissertation

Chapter 1: Introduction

This chapter provides an insight into the context of this dissertation. It mentions the growing predicaments in global inland lakes, the development of the concept for global endorheic lake changes, the main focus of this research, and the aims and objectives of this study.

Chapter 2: **Study area description and field investigation**

This chapter describes the Lake Turkana basin and the Aral Sea basin, comparing the changes occurring in the Lake Turkana basin to those that transpired in the Aral Sea basin. The results of the field investigations in both basins are presented here. Finally, the basin's socioeconomic and geographical characteristics, including geology, climatology, and demography, are described.

Chapter 3: Model description and data sources

This section details the land surface model that was used in this study. The model's data requirements, as well as the data sources, are enclosed. Additionally, this chapter discusses the preparation of the input data and the methodologies used to do so. Finally, the development of the Lake model to assess the changes in storage is also covered here.

Chapter 4: Detection of the current situation of irrigation

Chapter 4 discusses the development of methodologies for the detection of irrigation influences in an endorheic basin. The purpose here is to improve the methods for detecting irrigated areas and identifying salinized soils resulting from irrigation.

Chapter 5: Lake Turkana Basin Analysis

This chapter examines the changes in hydrological components in an endorheic basin for the past 18 years, from 2001 to 2018. The rationale for these changes is discussed, as well as the implications for the lake storage. Additionally, the developed endorheic lake model is employed to assess future water balance changes in the Lake basin. Here, the conclusions are drawn in light of the basin's current and expected future state.

Chapter 6: Assessing the threshold for sustainable changes in the endorheic basins

In this chapter, the threshold for sustainable changes in endorheic basins is assessed based on the volume and surface area variance. The changes in the Aral Sea are evaluated against those occurring in the Lake Turkana Basin. Conclusions in this chapter are based on the different instigated changes as observed in the endorheic Lake basins.

Chapter 7: Conclusions and Recommendations

This section summarizes the notable findings and makes some recommendations for future research.

Chapter 2

2 Study areas description and field investigation

This chapter describes the primary study areas in detail. Here, the various strategic aspects in both basins are compared and discussed. The timeline for the failure of the Aral Sea Basin's ecosystem services is reconstructed to determine the acceptable level of change in the Lake Turkana Basin.

2.1 Field investigation

2.1.1 Aral Sea Basin

In 2017, a two-week field study (from July 30th to August 14th) was conducted in Uzbekistan. This study included a salinity investigation along the Zeravshan River basin and a visit to the Amu Darya delta, one of the country's driest regions. The aim of this field study, which was done in collaboration with ICARDAs ICBA, was to determine the spatial gradation of salinity over time. It formed part of a follow-up to investigations made seven years earlier, between 2005 and 2010 by Khujanazarov et al. (2012). Additionally, another brief 3-day field visit was made in 2018 October, following attendance at a conference in the country.

At this time, the debilitating nature of irrigation activities in this basin was observed. First, the irrigation method used here is very water-intensive. As this investigation occurred during the irrigation season, cotton farms with overflowing furrows were observed (See Fig. 2.1-1 pg.8). This excessive water use inferred the poor irrigation efficiency that characterizes this basin. In fact, some studies estimate it to vary between 30 and 50 percent (Nazirov, 2005; Ryan et al., 2004). Additionally, due to the high heat capacity of water, these vast irrigated fields would be expected to modify the heat and water balance in this basin. A methodology

to detect the irrigated area in arid areas was developed through this difference in heat capacity (See chapter 4).

Fig. 2.1-1 Furrow irrigation in a cotton field in the Zeravshan River basin (August 2017)

Fig. 2.1-2 A poorly maintained transport canal with turbid water in the Zeravshan River basin (August 2017)

Fig. 2.1-3 A field with crystallized salts on the soil surface in the Amu Darya delta (October 2018)

Moreover, the transportation and drainage canals (See Fig. 2.1-2 pg.8) were observed to be poorly managed, subsequently influencing the lower irrigation efficiency due to reduced conveyance efficiency. In this arid and dry region, evaporation losses from these canals must be significant. It has been reported that the average evaporative rates in Central Asia are twice the precipitation received (Petr et al., 2004).

Additionally, some agricultural land plagued with salinity could be unmistakably spotted (See Fig. 2.1-3 pg.8). These fields were characterized by white salt crusts on the soil surface. Furthermore, it was noted that the spatial variation of these visible salts differed even within one farm, implying that the scale of accurate salinity detection could be much smaller than the farm scale. However, due to data insufficiency on the extent of salinity in the irrigated farms here, it was worth attempting to determine a cost-effective methodology for this (See chapter 4).

Finally, salinity measurement along the Zeravshan River revealed that salinity generally increased towards the downstream areas, similar to the previous reports by Khujanazarov et al. (2012). This gradation inspired the attempt for the remote sensing detection of salinity explained in chapter 4.

2.1.2 Lake Turkana Basin

A field study was conducted from October 26th to November 2nd in 2018 and October 15th to 20th in 2019. In 2018 a reconnaissance study along the Lake's eastern shows was conducted, including collecting salinity data along this region.

It was eminent that despite the damming of the Omo River and the subsequent filling of the Gibe III dam commencing in 2016, the Lake's water levels had significantly increased, inundating the adjacent areas. The damages caused to the environment following this could

effortlessly be identified. In some cases, small clasps of the (*Hyphaene compressa)* forests, locally known as the "Mukoma" tree, were dying out (See Fig. 2.1-4 pg.11). In others, properties near the Lake's shore were destroyed due to this rising Lake.

Additionally, the water quality, especially near the fishing centers, was quite abysmal. The expanding Lake had washed out animal droppings and fish remnants from the processing bay back into the Lake worsening the water quality (See Fig. 2.1-5 pg.12). This section of the Lake also tested highest for salinity compared to all observed points see points 3 to 5 in Fig. 2.1-6 pg.12.

Consensus attained through general talks to people from the local community revealed that the fishing stocks were dwindling, with some people attributing this to the rising Lake level. This revelation was unexpected as a previous study reported increased fish stocks with the rise in lake level (Mwikya, 2005).

The reliance on this Lake by the surrounding communities was also quite evident. Not only were populations of all ages observed conducting activities related to fishing along the Lake, but also community members were observed drawing water here. Although the lake's water is not palatable, it is widely used for other household water requirements such as cleaning.

During this reconnaissance study, the importance of observing the changes occurring in this Lake was reinforced. Therefore, water salinity sensors were handed to collaborators residing near the Lake to collect daily salinity data. However, this initiative failed after some months. Additionally, the data collected was inconsistent and supposed to be unreliable.

Consequently, in 2019, a meteo station was installed next to the Lake to collect valuable meteorological data, including; rainfall, temperature, humidity, wind speed, wind direction, and wind gust, for every 10 minutes (See Fig. 2.1-7 pg13. This data is transmitted remotely

and can be accessed in real-time. Moreover, a water level sensor was installed in the Lake to measure the lake level and water temperature. However, due to the current situation, this data has not been retrieved yet.

In summary, the field study conducted here illustrated the ongoing changes in this Lake and its surrounding.

- The increasing Lake level was causing the destruction of property and vegetation along the shore.
- The water quality, especially near the fishing centers, was relatively bad, with the highest salinity level of all observed points.
- The reliance on this Lake by the surrounding community was quite evident.
- Although data collection processes were instituted here, some of the data remain unavailable for use currently

Fig. 2.1-4 Inundated trees along the Lakeshore (October 2018)

Fig. 2.1-5 Poor water quality near a fishing center (October 2018)

Point	1	2	3	4	5	6	7
Salinity [g/l]	0.42	0.36	3.21	2.15	3.27	0.20	2.18

Fig. 2.1-6 Salinity gradation along the Lakeshore (October 2018)

Fig. 2.1-7 Meteo station installed next to the Lake (October 2019)

2.2 Background of the study areas

As mentioned in the previous chapter, due to alterations in global endorheic basins, the water and heat balance cycles in these basins have recently changed. These changes may be attributed to regional climate changes and anthropogenic activities (Bai et al., 2011; Olaka et al., 2010). Therefore, in the following sections, the focal basins are described highlighting the key factors contributing to alterations in the environments of these basins.

2.2.1 Aral Sea Basin

Fig. 2.2-1 The Aral Sea basin (Micklin, 2000)

First, the Aral Sea Basin is described, then changes that occurred here, and the reasons and implications for these changes are explained.

The Aral Sea Basin is a landmass in Central Asia comprised of seven countries: Uzbekistan, Turkmenistan, Tajikistan, Kazakhstan, Kyrgyzstan, Afghanistan, and Iran. Uzbekistan and Tajikistan have their entire territory here. Turkmenistan has the majority of its land within it. Two provinces of Kazakhstan and three provinces of Kyrgyzstan are located within this basin, and only the northern portion of Afghanistan and Iran is within it (CAWaterinfo, 2005a).

This basin covers over 1.8 million km^2, with an approximate total irrigated area between 75,000 and 79,000 km^2 (IFAS–UNEP, 2001). The Amudarya and Syr-Darya rivers are the primary sources of freshwater influx to the Sea. The Aral Sea Basin, depicted in Fig. 2.2-1 above, stretches between longitudes 56° and 78° east and latitudes 33° and 52° north.

Despite the extensive nature of irrigation areas, the irrigation efficiency in this basin is relatively low. Two components may be used to measure this performance: water conveyance and water application efficiencies (Irmak et al., 2011). Due to transmission losses, this basin has poor conveyance efficiency. Transmission losses in this basin are experienced when the amount of water delivered to the farm is less than the amount diverted from the source (Bekchanov et al., 2016; Micklin, 2000). These water losses are due to the lack of funds to maintain canals constructed during the Soviet period, resulting in water loss by canal seepage. Additionally, these canals lose water to evaporation in this arid and semi-arid region, reducing the conveyance efficiency.

On the other hand, water application efficiency is a measure of the proportion of total water supplied to a farm that is retained in the root zone to meet crop evapotranspiration needs (Bekchanov et al., 2016; Irmak et al., 2011). Thus, total irrigation efficiency is a feature of

both water application and conveyance efficiencies. Unfortunately, the overall irrigation performance of the basin's major irrigation schemes is abysmal.

According to some reports, it ranges between 30 and 50 percent (Nazirov, 2005; Ryan et al., 2004). Excessive water usage in the basin has resulted in the drying out of what was once the world's fourth-largest body of water. It is also one of the most significant causes of anthropogenic-induced climate change in Central Asia (Glantz, 1999).

According to Bucknall et al. (2003), water application rates in the basin are incredibly high, which has resulted in decreased farmland quality due to increasing water tables and salinization. Another study in Uzbekistan's Khorezm area found that irrigation water application increased groundwater levels, which led to secondary soil salinization (Ibrakhimov et al., 2007). These high water application rates have resulted in forced soil salinization in irrigation areas by adding 3.5 to 14 tonnes of salts per hectare per year (ibid.).

By 1994, around 40 percent of irrigated land in Central Asia was classified as saline (FAO, 2016a), and this figure is even higher today. For example, Toderich et al., (2008) reported that the lands affected by salinization in the Syrdarya province increased from 87 to 95 percent within five years. To avoid crop damage caused by salinity in irrigated soils, leaching water is used. Leaching is the application of water in surplus of the crop's evapotranspirative needs to wash salts out of the root region. In arid areas, leaching and drainage are required to maintain salt balance in the soil profile and improve crop yield. Leaching raises the water demand even further during the spring, when its normally carried out.

Irrigation is undoubtedly to blame for the Aral Sea's desiccation and the deterioration of environmental conditions in this basin. The state of the Sea and the seabed were directly affected by this desiccation. These effects included increased water salinity and exposure of

the sand and salts on the seafloor, resulting in sand and dust storms (Li et al., 2009; Micklin, 2010; Orlovsky et al., 2003).

Reduced sea area has effectively halted sea traffic, and increased salinization has suffocated the fishing industry. In addition, sand and dust storms have deteriorated the health of the residents of this basin, especially in the areas that border the Sea.

Currently, the Aral Sea Basin suffers from unsustainable water usage and widespread soil salinization, impairing the land's productivity. Additionally, the fishing industry has been dwarfed, and sea navigation has been reduced to a near-extinction level.

In conclusion, the Aral Sea basin changes can be attributed to the increase in irrigation areas. This unchecked irrigation area expansion has led to excessive water use and increased soil salinization.

2.2.2 The Lake Turkana Basin

In this section, the Lake Turkana Basin is described, dependency on Lake Turkana deliberated, and the ongoing changes in the basin discussed.

The Lake Turkana basin is approximately 156,000km^2 and is found primarily in Kenya and Ethiopia and to a smaller extent in Uganda and South Sudan. It stretches between longitudes 34° and 39° east and latitudes 0° and 10° north (See Fig. 2.2-2 below). Lake Turkana is located in a cross-boundary endorheic basin in Eastern Africa, surrounded by the arid lands of northern Kenya. The Omo, Turkwel, and Kerio rivers are the primary sources of freshwater influx to the Lake. The Omo River, which originates in Ethiopia, serves as the primary source of freshwater influx. It is estimated to provide 80-90 percent of the total inflow, with the Turkwel and Kerio rivers originating in Kenya providing the remaining 10-20 percent (Butzer, 1970).

The ecological value of the Lake and the lake basin, its importance in the local economy, and indigenous communities' dependence on it cannot be overstated (Obiero et al., 2016; The Oakland Institute, 2019). In Kenya, seasonal streams called "laggas" are essential water sources for communities in this arid region. During the dry season, indigenous communities near the Lake excavate shallow wells in these laggas to extract groundwater for consumption and domestic use (SeeFig. 2.2-3 to Fig. 2.2-5 pg.20). Moreover, the Lake serves as a major stopover for migrating waterfowl and is host to the Lake Turkana National Parks, a world heritage site (UNESCO, 2020). These parks are a grouping of three. Two can be found on the Central and South islands in the Lake, and one on the Lake's north-eastern shores. Lake Turkana and the Omo River are home to the world's largest Nile crocodile (*Crocodylus niloticus*) population (Obiero et al., 2016; UNESCO, 2020).

Furthermore, Lake Turkana is home to a diverse array of species. Such as hippopotamuses (*Hippopotamus amphibius*), the endangered Turkana mud turtle (*Pelusios broadleyi*), and a variety of venomous snakes (Obiero et al., 2016; UNESCO, 2020). Additionally, for well over a century, the communities around the Lake have relied on it for fish, initially for consumption but more recently as a source of revenue (Derbyshire, 2019; Kaijage and Nyagah, 2009). Furthermore, Lake Turkana has been home to a plethora of economically important fish species, including many tilapia species. Fishing is a significant economic practice in this basin's civilizations.

Over the past decade, the Lake Turkana basin has undergone drastic changes that have increased water demand (Hodbod et al., 2019; OTuRN, 2017). The need for economic growth and the ease with which financial resources can be obtained has resulted in an increase in damming of the Omo River, which is the primary source of water for Lake Turkana (Clack, 2018; IUCN, 2020; OTuRN, 2017). Among the most recent projects is the Gibe III dam. This

dam is the third in a series along the Omo River. It complements Gibe I and Gibe II, which have been in service since 2004 and 2010, respectively. This 200km^2 reservoir with a 14km^3 storage capacity was inaugurated in 2016 (Salini Impregilo, 2019, 2016). It aims to increase electricity production and expand land available for irrigation in the Omo River's downstream regions.

The irrigation area in the Lake Turkana basin has been growing due to the rising population, erratic rainfall patterns, a desire to increase crop production, and the ease with which financial resources for developmental projects can be obtained. Indeed, irrigation has been identified as a powerful tool for stimulating economic growth in Ethiopia. Additionally, there are plans to develop a 300 km^2 irrigation system on the Turkwel River, one of two rivers that drain into Lake Turkana from Kenya (Ondimu et al., 2018). However, these undertakings have increased concern about the impact of these large-scale projects on Lake Turkana's sustainability (Avery, 2012a, 2012b, 2010).

As seen in the above discussions, the Lake Turkana basin is rapidly changing. According to reports, large-scale irrigation schemes in the lower Omo river have the ability to extract up to 50 percent of the river water (Avery and Tebbs, 2018a). Although the Lake's current water levels have increased, this will no longer be the case in the future, especially if this water diversion continues unabated. In addition to many ensuing consequences, the groundwater in the basin will reduce, directly impacting the lives of thousands of residents here. The subsequent environmental catastrophe may be close to that experienced in the Aral Sea basin (Avery, 2014).

A comparison of irrigation, fishing, and health status in both basins will be elaborated on in the following pages, especially in light of the timeline for the failure of Aral Sea Basin’s ecosystem services. Since the Aral Sea Basin has already been transformed, a reconstruction

of the conditions that led to these changes can help advise on the level of acceptable change in the Lake Turkana Basin.

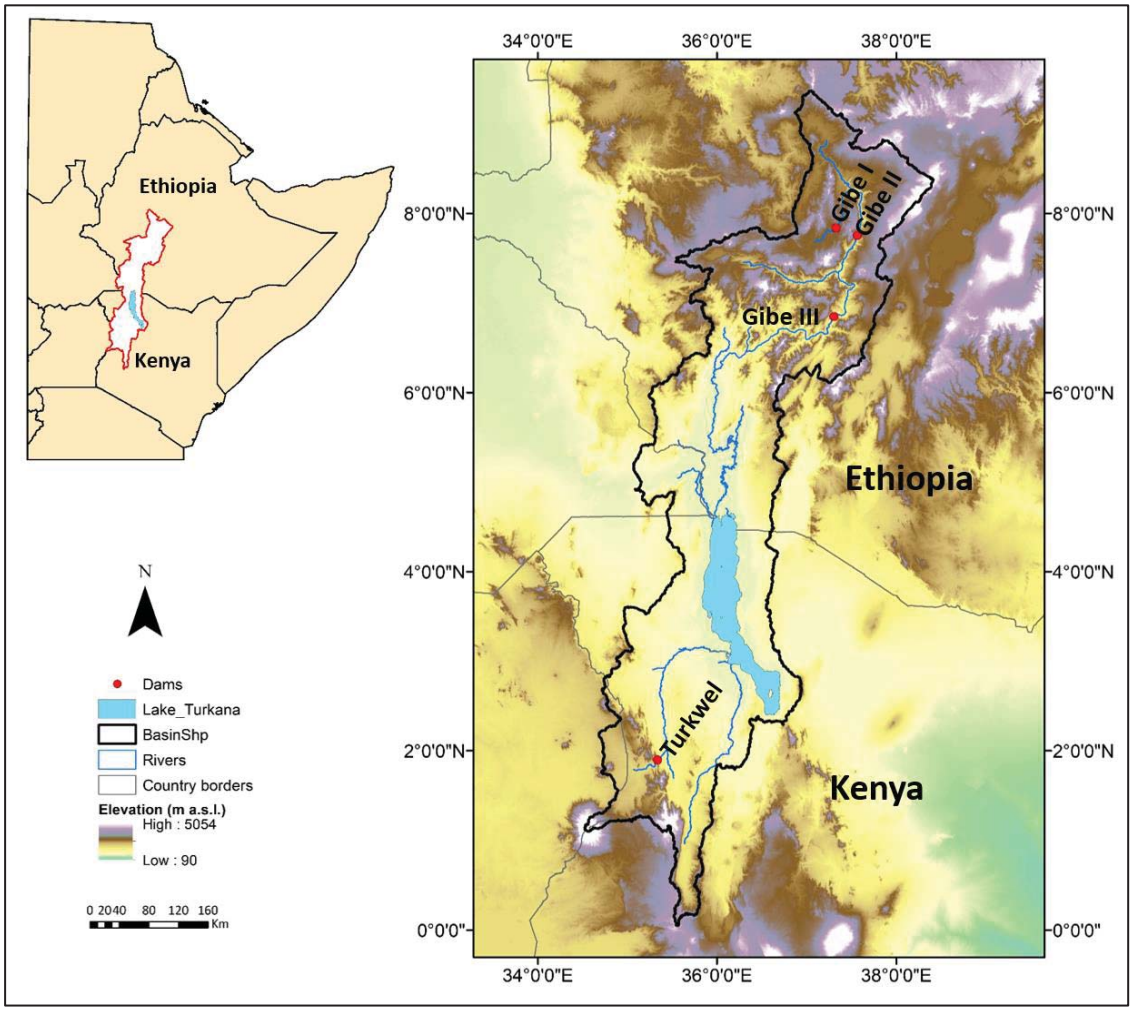

Fig. 2.2-2 Lake Turkana basin with elevation from the Shuttle Radar Topography Mission (SRTM)

Fig. 2.2-3 A Lagga during the wet season, the powerful streamflow is sufficient to move a truck

Fig. 2.2-4 A Lagga during the dry season, dry river bed with shallow groundwater

Fig. 2.2-5 A local community obtaining water from a shallow well in a Lagga during the dry season

2.3 Geography and topography

2.3.1 The Aral Sea Basin

The Aral Sea Basin is endorheic and landlocked. Here, the landscape and elevation vary from 0 meters above sea level near the Aral Sea to 7,500 meters above sea level in the east and southeast directions where the mountain ranges are found. This variation forms an excellent archetypal diversity of microclimate (CAWaterinfo, 2005b).

The Turan plain and the mountain zone are the two focal physio-geographic regions in this basin. This plain is a massive lowland that stretches through southwestern Kazakhstan, northwestern Uzbekistan, and Turkmenistan. In addition, two large deserts are located within this plain (CA Water, 2005; FAO, 2012). The Kara Kum desert in Turkmenistan, and the Kyzyl Kum desert in Uzbekistan and Kazakhstan, extend from the eastern part of the Caspian coast through the midsection of the Syr Darya River to the foothills of the mountain zone (ibid.). The eastern and south-eastern portions of the basin, on the other hand, are located in the Tien Shan and Pamir mountain ranges (ibid.). More than 50 percent of the desert covers the bulk of Kazakhstan, Turkmenistan, and Uzbekistan's territory, with mountains accounting for less than 10 percent of the total landmass (ibid.).

2.3.2 The Lake Turkana Basin

Much like the Aral Sea Basin, this basin is endorheic. However, this region does not have as much variation in elevation compared to that of the Aral Sea Basin. The elevation ranges from 350 meters above sea level near the Lake to approximately 4,500 meters in the northern and southern areas, where highlands and mountain ranges are located (see Fig. 2.2-2 above).

This basin is divided into various physiographical units with different characteristics, including escarpments, mountain ranges, plains, and swamps (JICA, 2012). Although this

endorheic basin traverses four countries, roughly half is in Kenya, while the other half is in Ethiopia. Lake Turkana, like the Aral Sea, is surrounded by arid and semi-arid lands. For this reason, it is described as the world's largest permanent desert lake. The Lake is located near the basin's midsection within the East African Rift.

2.4 Climatology

2.4.1 The Aral Sea Basin

The landlocked position of the Aral Sea basin contributes to its harsh continental climate, which is characterized by low and irregular precipitation (CA Water, 2005). Significant daily and seasonal temperature fluctuations, high solar radiation, and low humidity define this basin. Winters in Central Asia are harsh, with January temperatures averaging as low as -20° C in northern Kazakhstan. Conditions improve further south, but average midwinter temperatures remain below zero except in southern Turkmenistan and Uzbekistan (ADB, 2010). The basin's annual precipitation, including rain, sleet, and snow, is usually meager. On average, the deserts of Kazakhstan, Uzbekistan, and Turkmenistan receive less than 100 millimeters of precipitation per year. This precipitation steadily rises north, south, and east of the deserts on the steppes and plateaus. It is heaviest in the eastern and south-eastern mountains, with an average of 1,000 millimeters or more (ADB, 2010).

2.4.2 The Lake Turkana Basin

Due to its dynamic topography and proximity to the equator, this basin experiences one of Africa's most dynamic seasonal combinations (Herrmann and Mohr, 2011). The agro-climatic zones here range from cool and wet in the highlands to hot and arid near the Lake. Extended periods of intense diurnal winds characterize this region (Johnson and Malala, 2009). The annual precipitation in this region varies greatly as well, with the highlands receiving an average of 1400mm and the Lake receiving about 200mm. This region, unlike

the Aral Sea Basin, does not experience winter. Instead, it has a unimodal rainfall regime in the basin's northernmost reaches, a multimodal rainfall regime in the upper Omo River Basin, and a bimodal rainfall regime in the basin's southernmost reaches (Herrmann and Mohr, 2011). The mean annual temperature in this basin is relatively high, about 29°C (Passey et al., 2010).

2.5 Demography

Understanding demographic patterns within a region may improve our perception of the impacts of a population on the environment. Therefore, in the following subsections, the demography in the two focal basins is described.

2.5.1 The Aral Sea Basin

Central Asia's population grew from about 24 million in 1960 to nearly 74 million in 2019 (The World Bank, 2019a). This growth represents an increase of almost 208 percent. The population density in this basin is approximately 19 per km^2, with urban areas accounting for nearly 48 percent of the total population (Worldometer, 2021). Uzbekistan is the most populous of these Central Asian countries, with an estimated 33.6 million people, followed by Kazakhstan with 18.5 million, Tajikistan with 9.3 million, Kyrgystan with 6.5 million Turkmenistan with 5.9 million (ibid.) (See Fig. 2.5-1 pg.24). Undeniably, Central Asia has one of the highest per capita water consumption rates globally (The World Bank, 2017). Uzbekistan is the region's largest water producer, with annual water consumption of 58.9 billion cubic meters. Ordinarily, population growth has contributed to an increase in the water demand in this basin. Indeed, population growth increases the need for resources in the basin and the subsequent aggravated environmental impact. The population growth in this basin has been attributed to the reduction of water availability and deficiency in water quality (Peachey, 2004).

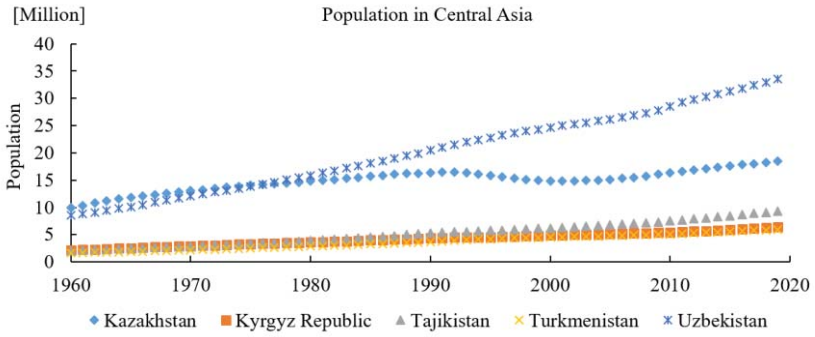

Fig. 2.5-1 Population increase in the Central Asia Republics from 1960 to 2019 (The World Bank, 2019a)

2.5.2 The Lake Turkana Basin

Turkana County, which encompasses most of the basin on the Kenyan side, has a population density of 14 per km^2. This population has been growing at 6.4 percent per year, with around 900,000 people reported to reside here in 2019 (KNBS, 2019; Turkana County Government, 2015). Since 2010, the Lower Omo River Basin population adjacent to the Kenya-Ethiopia border, near the northern part of the Lake, has been rising at 2.6 percent per year. (FAO, 2016b; SOGREAH, 2010; The World Bank, 2019b). In 2010, the population in this section was reported as reaching about 200,000.

Furthermore, the ongoing installation of development projects in this basin may trigger economic migration. This migration will result in a rise in population and resource demand. Therefore, it is essential to consider the population growth rate when planning for water resources management. This planning will ensure the availability and sustainability of the resource.

2.6 Irrigation area expansion and water use

Irrigation water, without a doubt, is a critical component of the hydrological cycle. In the following sub-sections, the changes that occurred in the Aral Sea Basin and those currently

ongoing in the Lake Turkana Basin are described. In addition, irrigation area expansion and the impending consequences from this are also clarified.

2.6.1 The Aral Sea Basin

The irrigation area in this basin increased steadily until about 1995, when the Soviet Union Republics collapsed. Water-intensive cotton was the main crop grown here for export. Fig. 2.6-1 below depicts the total irrigated area changes from 1960 to 2010. Due to this increasing area, the use of fertilizers, pesticides, and herbicides also grew. This, in turn, caused detrimental effects on the people's health and decreased water and air quality in this basin (See Health and Fishing and Salinity Sub-sections).

This expansion of the irrigation area had a significant effect on the volume and extent of the Sea, as more water was withdrawn for irrigation purposes. Fig. 2.6-2 below shows the relationship between increased irrigation area and reduced Sea area. The result of unchecked water abstraction is visible here. Between 1960 and 1970, a 13 percent rise in the irrigated area resulted in a 10 percent drop in sea level. By 1987, the Aral Sea split into two, the Large Sea and Small Sea, due to the continued water withdrawals from the rivers draining here. While the irrigated area increased marginally after 1995, increasing by only 2 percent, the sea area steadily shrank, reducing by 37 percent during the same era. The growing water demand might be a byproduct of the decreasing quality of farmland due to increased salinity, necessitating leaching, and changes in the regional climate, including increased frequency of scorching heat and dry weather (Glantz, 1999).

Indeed, the increased anthropogenic influences in this basin through the expansion of irrigated areas triggered one of the worst environmental catastrophes of our time. The effects from the growth of the irrigated area propagated a snowball effect distressing all aspects of livelihood for the people in this basin.

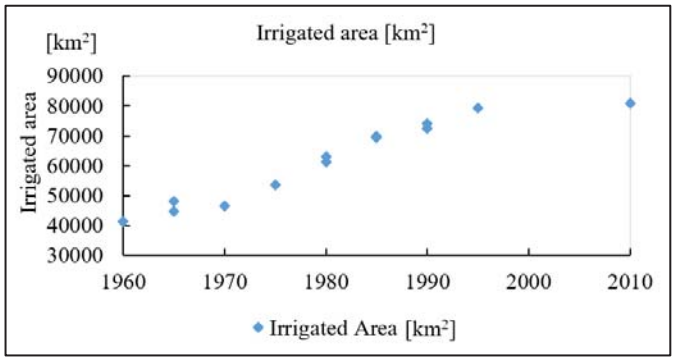

Fig. 2.6-1 Irrigation area expansion in the Aral Sea Basin from 1960 to 2010 (Glantz, 1999; Micklin, 2010)

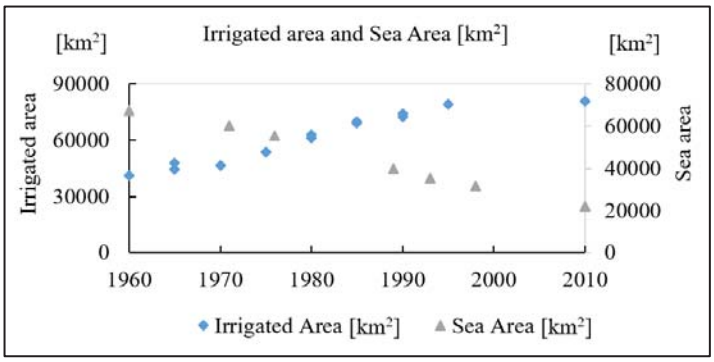

Fig. 2.6-2 Relationship between the Aral Sea area and the increasing irrigated area from 1960 to 2010 (Glantz, 1999; Micklin, 2010)

2.6.2 The Lake Turkana Basin

The Gibe III dam's construction enabled the regulation of streamflow in the Omo river. This dam has allowed the basin's irrigated area to expand. Ethiopian Sugar Corporation, a state-owned enterprise, announced plans to expand sugarcane cultivation in 2011. This project was expected to take 15 years to construct the irrigation canals and the excision of irrigation land. By establishing four sugar factories, the goal of the Kuraz Sugar Development Project is to create an integrated sugar development.

Initially, the project was expected to cover 1750km^2 (Avery, 2012b). However, this figure was revised to 1000km^2 (Government of Ethiopia, 2018). By 2016, only 106km^2 of land had already been cultivated, with an additional 130km^2 cleared (Kamski, 2016). Moreover, cotton irrigation is also established in this basin. Approximately 100km^2 of cotton is cultivated downstream of the Omo River, with an additional 400km^2 planned for expansion (Kamski, 2016).

In Kenya, there are plans to increase the irrigation area to propagate food security. Establishing a 300km^2 irrigation scheme in the lower reaches of the Turkwel river is part of this plan (Ondimu et al., 2018). Additionally, there are plans to establish a 100km^2 irrigation scheme at Todenyang, near Lake Turkana (Avery and Tebbs, 2018a). This scheme will help to mitigate drought effects and facilitate food security in this region.

With the continued expansion of the irrigated area in the Lake Turkana basin, increased abstraction of water to cater to the growing irrigation needs is expected. When this happens, declines in lake levels will be imminent, and an environmental disaster such as that of the Aral Sea Basin will be unavoidable.

2.7 Fishing and Salinity

When an Endorheic waterbody shrinks, the concentration of minerals increases as more water is evaporated from the Lake's surface. This phenomenon occurred in light of the shrinking Aral Sea. As a result, by the 1980s, the fishing industry here was almost non-existent. In this sub-section, the relationship between salinity and the fish stocks in Endorheic lakes is examined, highlighting the limit for the collapse of a previously thriving industry.

2.7.1 The Aral Sea

The fishing industry here flourished before the catastrophic shrinking of the Aral Sea began. In the late 1950s and early 1960s, this Sea accounted for roughly 7 percent of catches from all the former Soviet Union's endorheic lakes (Glantz, 1999). These catches represented about 48000 metric tons (Chen, 2018). Besides, 13 percent of the valuable fish species in the USSR were found here, including the large species, which made up 80 to 85 percent of the total catch (Glantz, 1999).

The diversity of the fish species here began to dwindle as the salinity in the Sea increased. This increase in salinity followed an inverse relationship with the volume of the Sea (See Fig. 2.7-1 below). By the 1980s, almost all the native species of this Sea had gone extinct, apart from the salt-tolerant ones. The fish species in this Sea reduced from about 20 species and seven subspecies to only four, two of which were accidentally introduced. The fishing industry collapsed when the Sea became increasingly salinized and more desiccated. By the mid-1980s, the fishing towns along the Seashores were reduced to ship graveyards, and economic turmoil struck. The overall catch from the Sea was zero in 1984, following the Sea's salinity rise to approximately 22 grams per liter (See Fig. 2.7-2 pg.29).

In 2005, the Kokaral Dam was built for remediation purposes, separating the Small Sea from the Large Sea and thereby increasing water levels. Increased water levels resulted in a drop in salinity from approximately 30 to 8 grams per liter, resulting in the return of nearly two dozen species of fish via the Syr Darya River (Chen, 2018).

As seen from the Aral Sea case, increased salinity negatively affects the fish stocks in an endorheic lake. When the salinity in the Sea got to 22 grams per liter, a total collapse of the fishing industry occurred. This information is crucial in understanding the limit of sustainable changes in an endorheic lake.

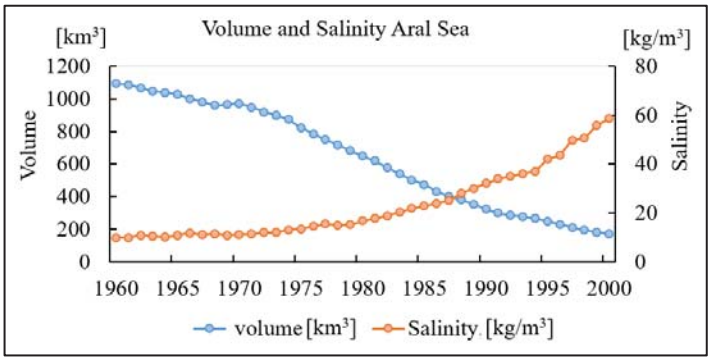

Fig. 2.7-1 The relationship between salinity and volume in the Aral Sea from 1960 to 2000 (CA Water, 2016)

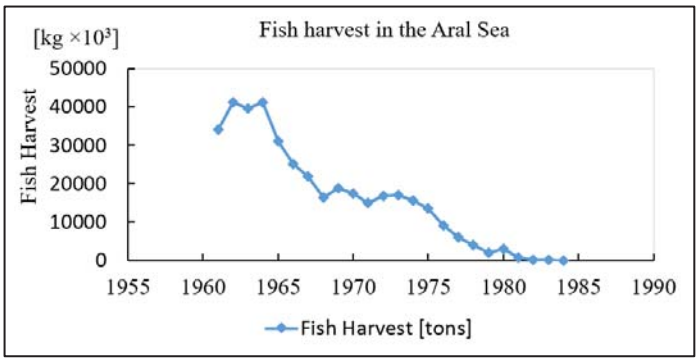

Fig. 2.7-2 The decreasing fish harvest in the Aral Sea from 1960 to 1984 (Micklin et al., 2014)

2.7.2 The Lake Turkana

Lake Turkana is the most salinized of all the Rift Valley lakes with natural fish fauna (Avery and Tebbs, 2018a). Here, the salinity level is estimated to be 2.5 grams per liter (Avery, 2012b). In the 1980s, this Lake was evaluated to sustain about 48 species of fish, 10 of which were endemic (Hopson, 1982). However, this figure had increased to 60 by the 2000s. The fishing industry here produces about 8000 metric tons valued at 6,000,000 USD (Malala et al., 2018). By 2016, about 7000 fishermen were reported to be operating here, with most of the communities living near the Lake engaging in fishing-related activities (ibid.).

The fisheries sector supports a thriving fish trade on both domestic and international markets, with a particular emphasis on the salted sundried dry fish trade to the Democratic Republic of Congo (ibid.). Since the fish in this lake breed in the shallow lake zones, the fish production here is highly related to the lake level. When the lake level decreases, salinity levels in these regions increase, impacting the fish stocks. The Ferguson Gulf, situated on the western shores, near the central part of the Lake, is one of the most important fishing grounds. In 1976, the tilapia production here was more than four times the harvest from the entire Lake (Mwikya, 2005).

Despite the Lake's current high level, a field study trip in 2018 discovered that the salinity level in the Ferguson Gulf was relatively high (See Fig. 2.1-6 pg.12). It was noted that the increase in the Lake levels resulted in the inundation of the regions surrounding the Lake, which contained grazing animal droppings and remnants of fish processing activities such as fish guts, thereby deteriorating the Gulf's water quality (See Fig. 2.1-5 pg12). Along the Lakeshore, carcasses of fish could be seen.

Even though the salinity levels in this Lake are significantly lower than those in the Aral Sea, there is growing concern about the impact of salinity on fish stocks. Moreover, the fishing industry here is quite sensitive to changes in the Lake's water level. As a result, any changes to the basin that affect the Lake's influx will undoubtedly affect the local fishing industry.

2.8 Health

Changes in the water level of an endorheic lake have been associated with detrimental health effects on the residents of these basins. Increased water level increases water-borne diseases, whereas decreased water level exposes the lakebed, resulting in more respiratory problems from the inhalation of toxic dust and salts. This problem is elaborated in the following sub-sections.

2.8.1 The Aral Sea Basin

A public health study in the regions near the seacoast from the 1970s to 1980s exposed the increase in various health-related problems (Glantz, 1999). One of the most notable discoveries was the increase in infant mortality with time. For example, around 60 percent of children under the age of one who perished in the Karakalpakstan region died of respiratory diseases, and 97 percent of these fatalities were from acute pneumonia (ibid.). Additionally, it was revealed that about 45.6 percent of children residing in this area were ill.

This increase in infant mortality was attributed to several factors, all of which were linked to changes in the environment caused by the expansion of irrigated areas and the modification of the region's micro-climate.

2.8.2 The Lake Turkana Basin

The communities surrounding the Ferguson Gulf are the most vulnerable when it comes to exposure to disease epidemics. Increasing lake levels have been reported to inundate the surrounding environment contaminating the water, leading to cholera outbreaks in this region (Carr, 2017; Luttah, 2020). A cholera outbreak here in 2020 infected 225 residents with one fatality (Luttah, 2020). Additionally, the residents here reported concern for visceral leishmaniasis (kala-azar) diseases (ibid.). These diseases are transmitted through the bite of sandflies. As the Lake's level increases, the sand surrounding the Lake is moistened, creating an ideal breeding ground for these flies.

An additional point of health concern is the high fluoride content in the Lake and groundwater in this region. The fluoride concentration in this Lake is greater than 10mg per liter (Hopson, 1982). This level is approximately ten times higher than the World Health Organization recommendation of between 0.5 to 1mg per liter. Despite this, it is one of the region's most vital water sources for humans and livestock. If the water levels in this Lake reduce, fluoride

enrichment will occur due to increased evaporation (Luo et al., 2018). In particular, some effects of chronic fluoride exposure are already eminent in this basin. These effects include a change in the hair color and browning of the teeth.

Therefore, fluctuations of water levels in a lake have far-reaching implications on the residents' health. Thus, understanding water circulation in a basin can also shed light on the imminent public health issues in a region.

2.9 Summary

In this chapter, the changes that occurred in the Aral Sea basin were described to highlight the expected changes in the Lake Turkana basin. The primary data source used here is the literature review of multiple studies. The objective for this was to identify changes occurring in endorheic basins by comparing Lake Turkana to the Aral Sea

- The expansion of the irrigated area in the Aral Sea basin has resulted in excessive water use. This growth has, in turn, propagated increased secondary soil salinization. By 1994, with approximately 79000km^2 of irrigated area, 40 percent of irrigated land in Central Asia was classified as saline.
- An inverse trend was established between the growing irrigated area and the reduction in Sea area. For example, when a 13 percent increase in the irrigated area occurred from 1960 to 1970, a 10 percent drop in sea level was experienced.
- Moreover, a similar inverse trend was described between the increase in salinity and reducing fishing stocks. When the salinity levels in the Sea got to approximately 22 grams per liter, the total collapse of the fishing industry occurred. At this level, only salt-tolerant fish could survive in the Sea.
- Finally, a reduction in the Sea level resulted in increased disease incidents in the Aral Sea basin. In the 1970s and 1980s, the Sea area had decreased by nearly half. During this

period, it was reported that approximately 60 percent of children under the age of one who died in the Karakalpakstan region died of respiratory diseases.

Chapter 3

3 Model description and data sources

In this chapter, the different data sources used are elucidated. Additionally, the model setup and the data preparation methods are clarified. Finally, the concept of the endorheic lakes water balance model, is presented.

3.1 Data Sources

This section is divided into four subsections, describing the data sources used in; identifying the current status of irrigated areas, initializing SiBUC LSM simulation conditions, developing the endorheic lakes storage change model, and future climate change projections. Table 3.3-1 pg43 shows a summary of all the data exploited in this study.

3.1.1 Data for identifying the current status of irrigated areas

The primary source of data for the identification of the current status of the irrigated area was derived from satellite products.

The land surface products from the Moderate Resolution Imaging Spectro-radiometer (MODIS) Terra satellite were applied here. This satellite collects daily global observations at approximate equatorial crossing time UTC 11:30 a.m., and 11:30 p.m. Land surface temperature (LST) and surface reflectance data were retrieved from the MOD11A1 and MOD09GA products.

MOD11A1 is a level 3 gridded product with a temporal resolution of 1 day and a spatial resolution of 1 km (Wan et al., 2015). The data for all the grids are from single clear sky observations. This data has been corrected for atmospheric conditions such as gasses, aerosols, and Rayleigh scattering (Vermote et al., 2011). This product was used to identify

irrigated areas by detecting the difference in heat capacity between irrigated areas and other land uses.

MOD09GA product, on the other hand, is a level 2 gridded (2G-lite[1]) product. It provides daily estimates of the surface spectral reflectance of the Terra satellite MODIS bands 1 through 7 at a 500m resolution. The bands are made up of the visible (band 1,3, and 4), near infra-red (band 2) and, short wave infra-red (band 5-7). Just like MOD11A1, this product has also been corrected for atmospheric conditions. This product was used to compute various indices for the detection of salinity in endorheic basins.

3.1.2 Data for Initializing SiBUC LSM simulation conditions

For the initialization of model dependant variables, the following data products were used.

Forcing data for the model was obtained from the Japanese 55-year Reanalysis (JRA-55) product, a project of the Japan Meteorological Agency (Kobayashi et al., 2015). It was developed through a comprehensive global atmospheric data assimilation covering a period of 55 years from 1958. It is the first product of its kind to use the four-dimensional variational analysis (4DVar) to eliminate model biases for this timeframe. Air temperature, specific humidity, air pressure, surface downwelling longwave and shortwave radiation, and wind speed were obtained from this product. The spatial resolution of the data is 1.25 degrees, while its temporal resolution is 3 and 6 hours. Precipitation data was obtained from the Global Satellite Mapping of Precipitation (GSMaP) version 6. Hourly-based precipitation is derived from satellite-borne passive microwave and infrared radiometers at 0.1 degrees spatial resolution (Ushio et al., 2009).

---

[1] Level 2G-lite provides a minimal level of compositing daily gridded level 2 data.

Land cover characteristics and soil and vegetation data were obtained from the European Space Agency (ESA) Land Cover (LC) product and ECOCLIMAP. ECOCLIMAP was used to initialize the LSM's soil and vegetation schemes. This dataset was created by combining current land cover and climate maps with Advanced Very High Resolution Radiometer data (AVHRR) (Masson et al., 2003). The clay and sand fractions in this product were derived from the FAO UNESCO soil map (FAO, 1988). This fraction of clay and sand served as a basis to classify the soil into the 12 main textures specified by the USDA for soil type interpretation. ESA LC was developed using a 300m Medium Resolution Imaging Spectrometer (MERIS) (Arino et al., 2000). It provides yearly changes to land use. ECOCLIMAP is available at 1km resolution, while the ESA LC is provided at 300m.

Additionally, data on irrigation area fraction was obtained from the Global Map of Irrigation Areas version 5, developed by Siebert et al., (2005). This product was generated by combining irrigation statistics with geospatial data on irrigation scheme location and extent. It is provided at a spatial resolution of 5 arc minutes. Here, it is used for identifying irrigated areas in the basin.

Finally, SRTM product from the United States Geological Survey (USGS) was used to provide the Digital Elevation Model (DEM) at a spatial resolution of 3 arc seconds for the derivation of topographical variables (Farr and Kobrick, 2000). MERIT Hydro flow direction product by Yamazaki et al., (2019) was used to delineate the lake basin. This product is derived from the MERIT DEM and inland water maps. It is also provided at a spatial resolution of 3 arc seconds.

3.1.3 Data for endorheic lakes storage change model

In this subsection, the data used to validate this model is described. Additionally, the procedure for deriving the Lake bathymetry is explained.

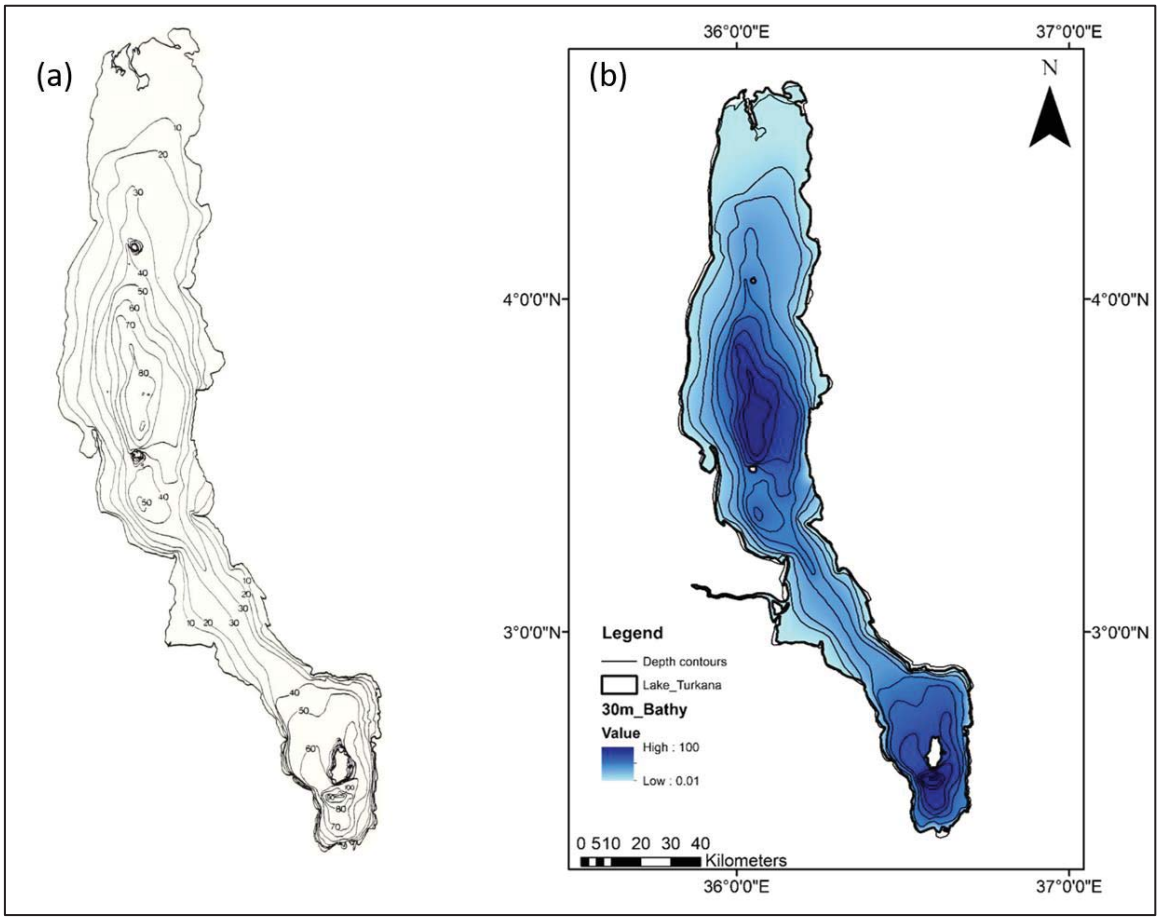

Fig. 3.1-1 Bathymetry map of Lake Turkana; (a) Lake Turkana depth contours by Hopson (1982); (b) Digitized bathymetry map for Lake Turkana with depth interpolation through the natural neighbor method

Altimeter data from the United States Department of Agriculture Global Reservoirs and Lakes Monitor (USDA G-REALM) was used to validate storage changes in the Lake. This product delivers time-series data of water level variations for some of the largest lakes and reservoirs in the world. It includes target height elevation in meters above mean sea level (m a.m.s.l.) and the satellite mean reference pass in meters. It is derived from the altimetry satellites Topex Poseidon, Jason-1, Jason-2, and Jason-3. This data set has been used widely

to evaluate lake level variations since the error presented by it is only to the order of a few centimeters.

Finally, bathymetry data was estimated by digitizing the bathymetry contour paper map provided by Hopson (1982). These bathymetry paper maps have been digitized in previous studies to provide ordered data sets (Nur et al., 2003; Sindhu et al., 2007). First, the contour lines for the lake depth were digitized, then geo-referenced and provided with the x,y,z dimensions. Next, the gradation of depth between the contours was interpolated using the nearest neighbor method. Finally, the derived bathymetry map gives an estimate of the lake depth at a 90m resolution (See Fig. 3.1-1 above).

3.1.4 Future projection data

A Global Circulation Model (GCM) from the sixth Coupled Model Intercomparison Projects (CMIP6) is used to assess the suitability of the developed lake model in projecting future changes to the Lake basin. For this, the GCM BCC-CSM2-MR from the Beijing Climate Center China is used. This model has a spatial resolution of 100km with the meteorological forcing variables at 6 hours and 3 hours. CMIP6 significantly expands upon CMIP5 in terms of the number of modeling groups involved, the number of future scenarios tested, and the number of different experiments performed (Hausfather, 2019). Shared Socioeconomic Pathways (SSP), SSP585, was selected for this study. This SSP presents high radiative forcing by the end of the century following a global forcing trajectory similar to RCP8.5. The data can be obtained from https://esgf-node.llnl.gov/search/cmip6/

3.2 SiBUC LSM description

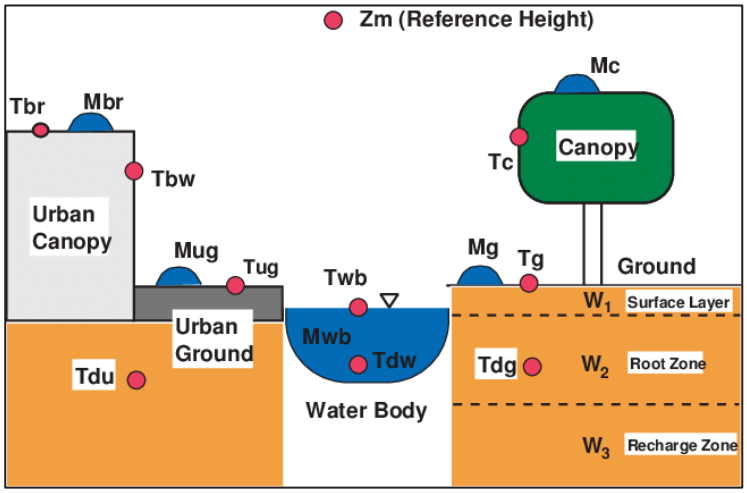

Fig. 3.2-1 SiBUC Land surface model (Tanaka, 2004)

The SiBUC LSM was developed by Tanaka and uses a mosaic parameterization scheme to incorporate different kinds of land uses into the model's land use scheme (Tanaka, 2005) (See Fig. 3.2-1 above). It is based on the Simple Biosphere (Sellers et al., 1986) and provides lower boundary conditions for sensible heat, latent heat, and momentum fluxes based on the grid-scale heat and water balance.

Each grid area is divided into three sub-schemes: green area, waterbody, and urban area. In the green area sub-scheme, there are 15 different land use classifications (See Table 3.2-1 pg.40), including irrigation land. This sub-scheme recognizes the mixed land uses in a grid, with the surface fluxes for each sub-model calculated separately. The fluxes in a grid are then calculated by weighting the average of the surface fluxes across each land use fractional area.

This model can consider artificial water operation in an irrigated mesh. Artificial water regulation is stipulated by the irrigation scheme in the green area sub-model. The irrigation scheme's basic principle is to keep the green area's soil moisture above the minimum required for each crop's growing stage.

Since the main crop under irrigation in this basin is sugarcane, spring wheat, class 12 was assumed to be the closest representation of the crop type

Table 3.2-1 SiBUC LSM land use classes

Classification	Land Uses
1	Broadleaf-evergreen trees
2	Broadleaf-deciduous trees
3	Broadleaf and needle leaf trees
4	Needle leaf-evergreen trees
5	Needle leaf-deciduous trees
6	Short vegetation/C4 grassland
7	Broadleaf shrubs with bare soil
8	Dwarf trees and shrubs
9	Farmland (non-irrigated)
10	Paddy field (non-irrigated)
11	Paddy field (irrigated)
12	Spring wheat (irrigated)
13	Winter wheat (irrigated)
14	Corn (irrigated)
15	Other crops (irrigated)

Soil moisture is of importance as a deciding factor for runoff generation and infiltration. The soil layers are divided into three categories in this model: surface layer, root zone, and recharge zone (See Fig. 3.2-2 pg.41). The model employs Richards' equation to redistribute soil moisture vertically in the soil sub-layers. Darcy's law is used to consider vertical moisture movement.

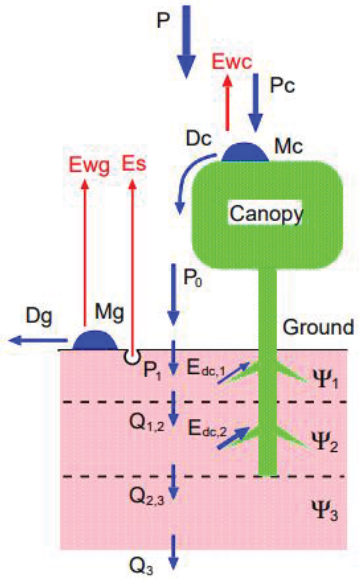

Fig. 3.2-2 Schematic image of interception

In this model, the maximum store on the ground *(Sg)* and the maximum store on the canopy *(Sc*) are set. When the intercepted water store on the canopy *(Mc*) exceeds the *Sc*, drainage from the canopy *(Dc)* less *Sc* occurs. This *Dc* becomes the effective precipitation P_0. If the soil is saturated, and the intercepted water store on the ground (*Mg)* exceeds *Sg*, then runoff (*Dg)* less *Mg* occurs. However, if the soil is not saturated, some of the P_0 can infiltrate into the soil layer if P_0 is stronger than the hydraulic conductivity at saturation (K_s). In this case, infiltration excess runoff occurs. This is shown in Eq (1);

$$P_1 = P_0 \quad \text{When } P_0 \leq k_s$$
$$P_1 = k_s \quad \text{When } P_0 > k_s \qquad (1)$$

Once the water infiltrates, it is redistributed vertically between soil layers using the Richards equation with forcing terms for evapotranspiration and infiltration, as shown in Eq (2).

$$\frac{\partial W_1}{\partial t} = \frac{1}{\theta_s D_1}\left[P_1 - Q_{1,2} - \frac{1}{\rho_\omega}\left(E_s + E_{dc,1}\right)\right]$$

$$\frac{\partial W_2}{\partial t} = \frac{1}{\theta_s D_2}\left[Q_{1,2} - Q_{2,3} - \frac{E_{dc,2}}{\rho_\omega}\right] \quad (2)$$

$$\frac{\partial W_3}{\partial t} = \frac{1}{\theta_s D_3}\left[Q_{2,3} - Q_3\right]$$

Where,

W_1 , W_2 , W_3 : Soil moisture stores in the surface layer, root zone, and recharge zone.
t: Time
D_1 , D_2 , D_3 : Depth of Surface layer, root depth layer and recharge layer
$Q_{1,2}$: Infiltrated water from the first layer to the second layer
$Q_{2,3}$: Infiltrated water from the second layer to the third layer
Q_3 : Infiltrated water from the third layer
$\rho\omega$: Density of water
Es : Direct evaporation of water from the surface soil layer
$E_{dc,1}$, $E_{dc,2}$: Abstraction of soil moisture by transpiration
θ_s: soil water content at saturation

3.3 Description of the developed endorheic lakes water balance model

In this model, the change in lake storage is assessed through the inflow generated by the SiBUC LSM. The lake level is determined by the altimeter satellite for the first timestep. After that, the new lake level is estimated by computing the change in storage for each centimeter, until the calculated storage is comparable to the analyzed water balance.

As a result, if the Lake's inflow exceeds its evaporative losses, it is said to expand. The new lake level is then estimated, which would reflect the newly inundated meshes. Subsequently, the land use class of the inundated meshes is then modified to reflect the new waterbody. The converse is true for a shrinking lake. In this case, the desiccated meshes are assigned the dominant land use class surrounding the Lake, shrubs with exposed soil. Finally, these newly reassigned land use classes are updated and employed to simulate the next time step using SiBUC LSM.

Table 3.3-1 A summary of the data products used in this study

	Data Product	Parameters	Frequency	Resolution	Data source
1	MOD11A1	Land Surface Temperature	1-day	1km×1km	https://search.earthdata.nasa.gov/search
2	MOD09GA	NDWI	1-day	500m×500m	https://search.earthdata.nasa.gov/search
3	JRA-55	Meteorological forcing	3-hours, 6-hours	1.25°×1.25°	http://search.diasjp.net/en/dataset/JRA55
4	GSMaP	Precipitation	1-hour	0.1°×0.1°	http://hokusai.eorc.jaxa.jp/
5	ECOCLIMAP	Soil and vegetation	Single data (soil) Single10-day data (Vegetation)	30sec×30sec	http://www.cnrm.meteo.fr/gmme/PROJETS/ECOCLIMAP/page_ecoclimap.htm
6	ESA LC	Land cover characteristics	Yearly	300m×300m	http://maps.elie.ucl.ac.be/CCI/viewer/download.php
7	Global Map of Irrigated Areas	Irrigated area fraction	Single date	5min×5min	http://www.fao.org/aquastat/en/geospatial-information/global-maps-irrigated-areas/latest-version/
8	SRTM	Digital elevation model	Single date	90m×90m	https://search.earthdata.nasa.gov/search
9	MERIT Hydro	Flow direction	Single date	90m×90m	http://hydro.iis.u-tokyo.ac.jp/~yamadai/MERIT_Hydro/
10	USDA G-REALM	Lake surface elevation	10-day		https://ipad.fas.usda.gov/cropexplorer/global_reservoir/Default.aspx
11	MOD09A1	NDWI	8-day	500m×500m	https://search.earthdata.nasa.gov/search

Chapter 4

4 Detection of the current situation of irrigation: Aral Sea

As discussed in the previous chapters, irrigated area is critical to consider as it affects water and heat balance in endorheic basins. Additionally, implications of these anthropogenic-induced alterations can result in widespread destruction, as explained in chapter 2. Thus, it is critical to ascertain the status of irrigated areas (both their scale and condition) in order to comprehend their implications within a basin. In this chapter, the methodologies to detect the current status of irrigated area is described. Since the Aral Sea Basin is among the world's largest irrigated zones, This chapter is based on this basin.

4.1 Background of the study

The primary irrigation system in the Aral Sea basin is furrow irrigation. However, this technique is very water-intensive, and its use in this basin culminated in the desiccation of the Aral Sea. Furthermore, irrigation has resulted in the salinization of soil. In particular, irrigation water naturally contains some dissolved salts, and when plants consume this water, salts accumulate, resulting in primary soil salinization. Additionally, secondary soil salinization is becoming more prevalent as a result of excessive water application. This water application elevates groundwater levels, bringing dissolved salts closer to the soil surface. These salts then collect in the soil as a result of evaporation leading to secondary soil salinization.

Ordinarily, due to the basin's ongoing environmental challenges, the actual irrigated areas differ annually, not merely due to annual climatic fluctuations but also as a technique for farmers to respond to irrigation-related problems. Therefore, the challenges in estimating the actual irrigated area in this basin and suggested solutions are discussed in the following

subsections. Moreover, methods for detecting soil salinity and the problems associated with this are also investigated.

4.2 Detection of irrigation area

Despite the continued expansion of irrigated areas to meet global food demand, this irrigated land's spatial extent and distribution remain unknown (Vörösmarty, 2002). Besides, the currently available maps are primarily based on country-level statistics, which may be out of date, underestimated, or constructed using data with coarse resolution (Droogers, 2002; Molden, 2000).

Central Asia is a region marked by rapid changes in land use. Accurate estimation of irrigated areas, on the other hand, is challenging. Moreover, this estimation is challenging because data collection across a large territory, particularly in developing countries, is complex.

Numerous attempts have been made on a global scale to ascertain the spatial extent of irrigated areas. One such example is the United States Geological Survey's (USGS) Global Land Cover Characterization (GLCC) map (Loveland et al., 2000). However, in this product, the irrigated area is identified in four broad categories. Therefore apart from being static, the irrigated areas are not isolated but form part of a more general classification. The provided land cover classification, therefore, does not reflect land cover in this dynamically changing region. Notably, during drought or dry years, the non-irrigated area may be erroneously classified as irrigated.

Another example of a land cover product with irrigated classes is the European Space Agency's (ESA) global land cover product (Arino et al., 2000). However, the irrigated area in this product is also included in several broad thematic classes.

Granted, several studies have successfully assessed the spatial extent of irrigated areas at the regional scale using climate and vegetation-derived indices. Crop mapping using NDVI revealed that irrigated crops maintain higher NDVI than the non-irrigated ones for most of the growing season, allowing the two to be distinguished (Wardlow et al., 2007). Furthermore, Gumma et al. (2014) used NDVI to accurately capture the seasonal variability in Bangladesh's rice crop. Ozdogan (2008) reported a high accuracy in mapping irrigated areas in the dryland Western United States using a multi-instrumental technique, employing both climatic (climatological moisture index) and vegetation (NDVI) indices. However, identifying the drought effect using vegetation indices such as NDVI is difficult. This information was reported in a study on drought monitoring, which concluded that the time lag between NDVI and precipitation is approximately one month, rendering this index unsuitable for drought monitoring without regard for the time lag (Wan et al., 2004). Additionally, some indigenous plants in the Aral Sea basin have roots that extend up to 30 meters. Since the groundwater level in the delta is high, indigenous plants thrive here, making it challenging to separate irrigated and non-irrigated areas using NDVI.

Previously, a simple index based on satellite land surface temperature (LST) was developed to detect irrigated areas in the Aral Sea Basin (Mbugua, 2018). However, climatology and topographical influences on LST were not isolated. Therefore, this study aimed to improve the detection of irrigated areas in this arid region using the SiBUC LSM analyzed radiative temperature and satellite-based LST. Since the effect of irrigation is already captured by the satellite's LST, the model simulation of LST is performed with and without considering this effect to test out the most ideal irrigation area detection method. The central hypothesis behind these methods is the difference in heat capacity between soil with high moisture and drier soils.

Therefore, the main objective of this study is to improve the detection of irrigation areas in arid regions by developing LST-based indices derived from satellite data and LSM.

The following subsections expound on the specific study area, development of the concept, and validation method utilized.

4.2.1 Amu Darya delta, Aral Sea Basin

The area of focus here is the Amu Darya delta, depicted in Fig. 4.2-1 pg.48. This delta is located in the Karakalpakstan republic of Uzbekistan and partially in Turkmenistan. Tuyamuyun dam, the primary source of data for validation, is found here. This dam was built primarily to provide irrigation water and is located in the upper reaches of this delta. This delta is positioned in the driest region of Uzbekistan and has a long history of drought.

In this region, droughts in 2000, 2001, and 2008 triggered the drying up of numerous artificial reservoirs in Karakalpakstan, resulting in severe water shortages for irrigation and drinking (Eurasianet, 2016). Subsequently, approximately 90 percent of the rice crop and 75 percent of the cotton crop were destroyed in 2000 and 2001 (Frenken, 2012). Furthermore, in terms of irrigation water demand, this delta is situated in one of the most vulnerable areas to climate change in the Aral Sea Basin (Touge et al., 2015).

This area is also severely affected by secondary salinization due to increasing water levels resulting from high water application rates. According to Ibrakhimov et al. (2007), secondary soil salinization is adding an average of 3.5 to 14 tons of salt per hectare per year in the Khorezm region of Uzbekistan's Amu Darya delta.

Fig. 4.2-1 Amu Darya delta in Aral Sea basin (Micklin, 2000)

4.2.2 Development of irrigation detection indices

The developed irrigation area detection methods were based on the following concept. Since water has a higher heat capacity than soil, soil with a higher moisture content does not react immediately to temperature changes. Moreover, the increased evapotranspiration caused by irrigation water decreases the LST in irrigated areas during the day. This is because water absorbs heat from the surrounding in order to change the state from liquid to gas. Therefore evaporation of water has a pronounced cooling effect. Here the LST provided by the satellite is assumed to represent the actual land conditions. In contrast, the SiBUC LSM provided LST is considered to be the predicted ideal LST in both states, with and without irrigation.

The primary purpose of using the model to simulate LST is to remove the influences of climatology and geological variability on temperature. Therefore, when simulating irrigation conditions, the mesh was assumed to be fully irrigated. Conversely, when simulating conditions without irrigation, the mesh was considered to be fully unirrigated. As the satellite detects LST, it provides the surface temperature for actual ground conditions, including precipitation influences. Therefore, the irrigation-generated effects on satellite LST are not

sequestered. Furthermore, topographical differences on satellite LST make it challenging to detect irrigated areas in these regions.

Admittedly, LST is challenging to estimate and validate both in satellite data production and model simulation. This is because LST is influenced by many factors and requires the knowledge of many influencing parameters (Copertino et al., 2012). However, the model's irrigation scheme is integrated with topography and climate-linked parameters in deciding the irrigation water requirement. Therefore, the simulated LST is sufficient for isolating the effect of reduced temperature caused by irrigation and eradicating climatic and geological influences. The actual (satellite-based) and ideal (LSM-based) LSTs are used in this analysis to disentangle anthropogenic effects on LST.

4.2.3 Irrigation indices

The following Eq.(3-(5) below were applied to develop LST-based indices (R_1 – R_3) in an attempt to detect the irrigated area in the Amudarya delta.

$$R_1 = \Delta ST_{SAT} - \Delta ST_{LSM\_NI} \tag{3}$$

$$R_2 = \frac{ST_{SAT}^{day} - ST_{LSM\_NI}^{day}}{ST_{LSM\_IR}^{day} - ST_{LSM\_NI}^{day}} \tag{4}$$

$$R_3 = \frac{ST_{SAT}^{day} - ST_{LSM\_NI}^{day}}{AveST_{SAT}^{day} - AveST_{LSM\_NI}^{day}} \tag{5}$$

where, R_1 to R_3 depicts the irrigation indices, ST is the surface temperature, ΔST is the surface temperature difference between day and night, $AveST$ is the long-term average of surface temperature. And suffix SAT denotes observed by satellite, LSM_IR and LSM_NI,

indicates simulated with full irrigation and without irrigation, respectively, and day means daytime.

Eq.(3) above was used to remove the climatic influences and the topographical differences that may affect ΔLST, to identify the irrigation effect in a mesh. To isolate the irrigation effect, simulated LST by the LSM without considering irrigation is subtracted from the satellite LST representing the actual conditions observed in the study area.

Eq. (4) compares the irrigation effect observed by the satellite with the ideal simulated irrigation effect. Since this is the rate of the actual irrigation effect from the ideal irrigation effect, it would reflect the irrigation fraction in the mesh.

Eq.(5) compares the irrigation effect observed by the satellite with the average simulated irrigation effect. This can be used to detect a drought event by comparing the irrigation effect in a given year to that of an average year. The annual irrigation variability between a given year and an average year is highlighted with this third index.

4.2.4 Irrigation effect on LST portrayed by the LSM

Fig. 4.2-2 pg.51 shows monthly changes of LST in 2001 at 4 pm local time at a farm in the delta. This figure is based on the LSM simulation of LST with and without the consideration of irrigation. At the beginning of the year, the simulated LST for both cases exhibits a similar trend. However, during the irrigation season from March to September, the simulated LST considering irrigation drops by approximately 5 degrees before resuming a similar trend towards the end of the year.

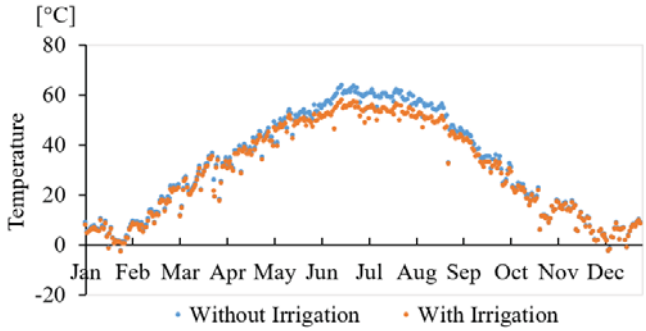

Fig. 4.2-2 LST changes by LSM at 4 pm local time in an irrigated farm in the delta

4.2.5 Detecting drought using LST

During the irrigation season, LST can be used to detect a drought year or a dry year. Such a year is characterized by scarcity of water leading to the abandonment of some irrigation land. Fig. 4.2-3 pg.52 shows a time-series analysis of the difference between day and night time LST by the satellite in an irrigated mesh in the delta. Here, an approximate difference of 4 degrees can be seen between an average year and a drought year. A 30 point moving average is used to show the trend in LST in both a drought year and an average year.

When cotton irrigation is typically carried out between June and October, a significant drop in temperature is observed. The temperature then remains relatively stable until the end of summer, when it begins to decline again. During the irrigation season, this difference in LST between day and night time is approximately 20^{o}C in 2001, a drought year, and 16^{o}C in 2017, an average year. Due to the satellite's much coarser spatial resolution compared to the size of the farms in this region, the fraction of irrigated area is much larger near the water source and decreases as one moves further away. Therefore, irrigated areas will have a lower LST closer to the water source than much further away.

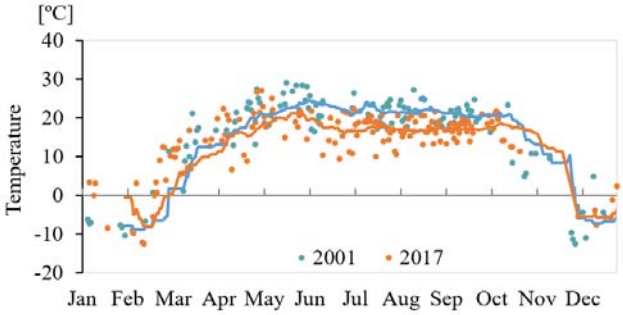

Fig. 4.2-3 Changes in the difference of day and night time LST by the satellite at an irrigated farm at the delta

Fig. 4.2-4 pg.54 shows the potential of the three indices in detecting the drought effect in irrigated areas during the irrigation season. Due to water scarcity during a dry year, the irrigation fraction further away from the water source is reduced, resulting in a higher LST, as shown below. The indices were computed from a 10-day average of LST data for the years 2001 and 2017.

Fig. 4.2-4 (a-c) pg.54 shows a higher value for all the indices in the month of August 2001, especially in the northern part of the delta compared to (d-e). In 2001, some areas in the northern region of this delta were severely affected by drought and could not be irrigated.

Therefore, the proposed LST indices can distinctly depict this decrease in irrigated areas. R_1 illustrates changes in the irrigated area due to anthropogenic influences, which relate to a reduction of the irrigated area due to drought.

R_2 appears to be directly related to irrigation fraction and thus has a more prominent effect on drought impact than R_1 or R_3. This index compares the ideal simulated influence of irrigation (from the model) and the actual irrigation condition (from the satellite).

R_3 appears to be the least applicable of the three indices because it compares the actual irrigated conditions to the average changes over time. However, this average change computation may include drought years in the past, which might affect the results.

To validate the indices' idealness in detecting changes in irrigated areas, a comparison with the outflow from the Tuyamuyun dam was made. First, the total volume released from the dam in August for some 11 years (2001 to 2011) was calculated. Then the sum of the three indices for all meshes in the delta for the same period was computed. Finally, the two calculated values from the three indices and the dam were compared.

The results reflect the ability of these three indices in detecting irrigation in the delta. Fig. 4.2-5 (a) shows the average computed value for R_1 compared with the dam water released, while (b and c) show the calculated sum of R_2 and R_3 compared with the same.

A similar trend can be seen between the water released and the indices. The higher the volume of water released for irrigation, the lower the value of the index. Drought occurrence in 2001 and 2008 is also clearly indicated by these indices. However, since this analysis involved only the summation of indices, the result may be affected by meshes with extreme value. For further research, the irrigation fraction of all meshes needs to be analyzed more precisely and verified by local data to elucidate this. The month of August had the best results of 5 irrigated months observed (May to September)

4.2.6 Summary

In this study, the irrigated area is detected using LSM and satellite LST. The idealized LST was computed by the LSM, while the actual LST was provided by the satellite. The use of idealized LST was necessary to eliminate climatic and topographical influences on LST to identify anthropogenic influences (irrigation).

Water volume data from the Tuyamuyun dam provided a comparable representation of water availability in this drought-prone delta. However, due to the difference in heat capacity between water and soil, it was expected that soil with high moisture content would not

respond immediately to temperature changes. Therefore, three indices were developed to detect the irrigated area based on this property.

The results show the potential of the indices to detect irrigated areas and the effect of drought on this area. The irrigation fraction was observed to be lower during a drought year as compared to an average year. This reduced fraction was especially true further away from the water source due to water scarcity.

The indices' competency in detecting irrigation in the delta was further confirmed by the discernible trend between these indices and the dam's water release.

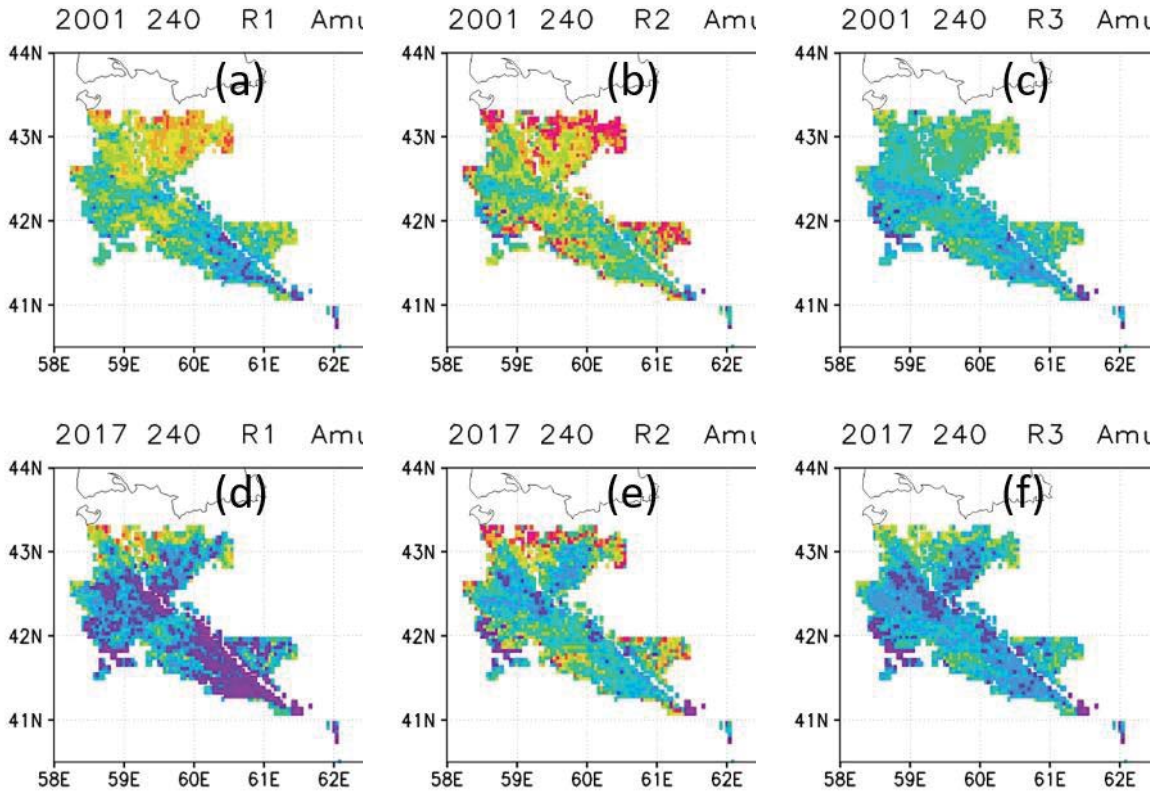

Fig. 4.2-4 Effect of drought on LST in the irrigated area; (a) LST index R_1 in August 2001 ; (b) LST index R_2 in August 2001; (c) LST index R_3 in August 2001; (d) LST index R_1 in August 2017 ; (e) LST index R_2 in August 2017 ; (f) LST index R_3 in August 2017

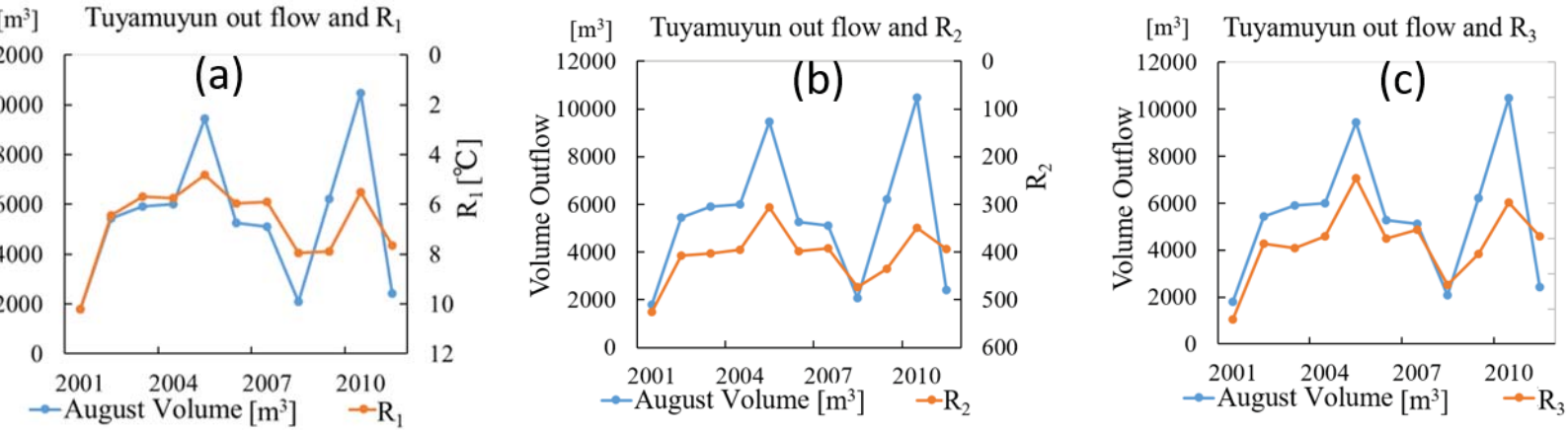

4.2-5 Comparison of Tuyamuyun dam water volume released in August and the three indices ; (a) R_1 and dam outflow ; (b) n outflow ; (c) R_3 and dam outflow

4.3 Detection of salinized soils

As highlighted in the background section of this chapter, soil salinization is a growing problem in the Aral Sea Basin. Indeed, Central Asia is one of the world's most severely affected regions by the salinization of irrigated land (Owens, 2001). According to Toderich et al. (2008), land affected by salinization, particularly human-induced, increased from 87 to 95 percent in the Syrdarya province within five years. Of these affected soils, more than 80 percent were considered heavily salinized. Another study by Bucknall et al. (2003) reported that the water application rates in this basin are incredibly high, leading to a reduced quality of farmland through rising groundwater tables and induced soil salinization. Ibrakhimov et al. (2007) described the consequences of rising groundwater in Uzbekistan's Khorezm region. On average, secondary soil salinization adds between 3.5 and 14 tons of salts per hectare per year.

Fig. 4.3-1 (a) below shows a farm with accumulated salt on the soil surface due to high groundwater levels and (b) shows leaching water applied to a farm in Karakalpakstan located in the lower Amu Darya delta. In order to prevent salinity in the soils from affecting crops, leaching water is applied. This process further increases the water demand during spring, when it is usually carried out. In highly saline regions such as Karakalpakstan, leaching water accounts for one-third of the total water use (Bucknall et al., 2003).

By the end of the twenty-first century, drought days are expected to increase by more than three times in most parts of Central Asia, despite the region's aridity (Hirabayashi et al., 2008). Therefore, because leaching and drainage are required to maintain the salt balance in the soil profile and sustain crop yield in arid areas, an accurate estimate of the extent of salinized soil is necessary for environmental preservation and economic growth planning.

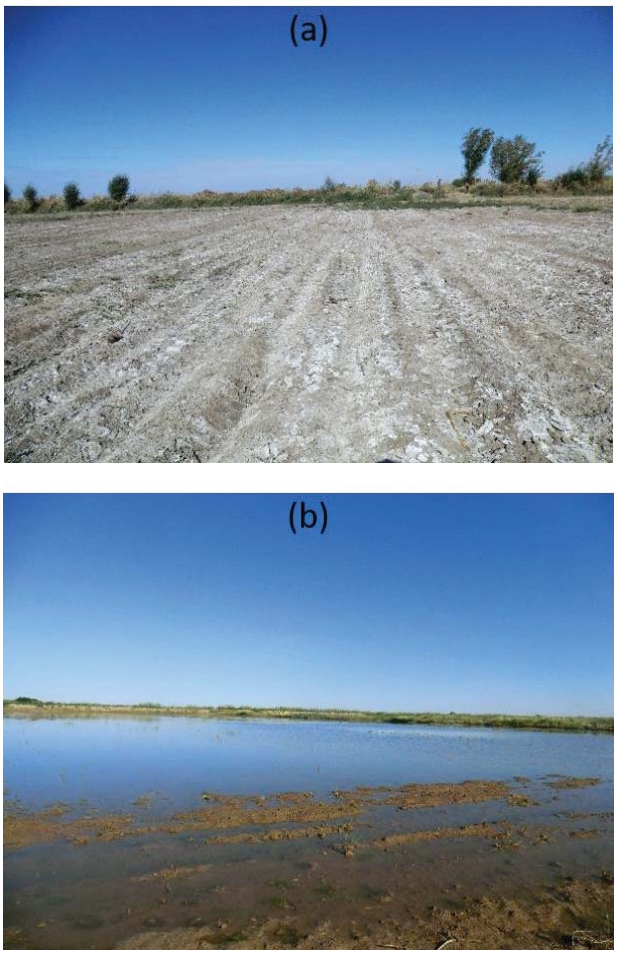

Fig. 4.3-1 Salinity induced problems in the endorheic Aral Sea basin; (a) Crystalized salts in a farm; (b) Leaching water applied to wash out salts from the soil surface

Despite this, FAO (2016) reported that assessing salinization in this region was challenging even at the national level, and very little information on the subject could be found. Still, according to Khujanazarov et al. (2012), salinity levels increased over time and from upstream to downstream regions in the Zeravshan river basin, as illustrated in Fig. 4.3-2 below. This gradation in salinity is attributed to salt load in return flows from irrigated areas discharged via collector drains, which are typically neglected.

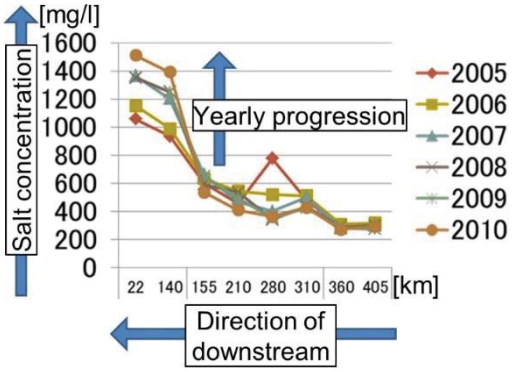

Fig. 4.3-2.Salinity gradation in the Zeravshan River (Khujanazarov et al., 2012)

The conventional method of determining soil salinity involves collecting in-situ soil samples and analyzing their solute content and electrical conductivity in the laboratory. However, this method is both expensive and time-consuming. Remote sensing techniques are therefore being progressively applied for the monitoring and mapping of these saline soils. Furthermore, they provide an invaluable opportunity for detailed spatial and temporal observations of irrigated area variability and soil salinization. Hence, remote sensing techniques demonstrate the possibility of overcoming the regional lack of information on water management (Conrad et al., 2007).

Remote sensing analyses for the detection of salinized soils have been carried out using various techniques worldwide. These include developing indices based on thermography, spectral reflectance, and vegetation conditions. These salinity detection methods can be broadly categorized into direct and indirect methods (Metternicht et al., 2003). Direct methods involve the reflectance of the bare soil, while indirect methods involve assessing vegetation type or condition. A study by Wang et al. (2002) using the Simple Ratio Vegetation index (SRVI) reported an indication that canopy reflectance in the near-infrared spectral region was reduced incrementally with increasing levels of salt stress. Wiegand et al. (1994) related NDVI to crop yield and noted that cotton lint yields decreased by 43 ± 10

kg per hectare for every 1 dS/m increase in salinity. Lobell et al. (2010) predicted the ground estimates of EC using only averaged Enhanced Vegetation Index (EVI) and reported a correlation of R^2 between 0.21 and 0.37. Several assessment studies on salinity have used salinity and vegetation indices with varying levels of success in their analysis.

Remotely sensed spatial and temporal variability of salinity was not exhaustively discussed in Mbugua (2018). Therefore, in this study, the primary aim was to improve this discussion, and highlight the possibility of using existing salinity detection methods to assess this spatial and temporal variability of salinity in endorheic basins.

Therefore, this study aims to elucidate the capability of remote sensing in detecting soil salinity in endorheic basins.

The following subsections describe the study area, methodology including the salinity indices employed, and results of this study. Here, salinity was not measured directly from the farms. Instead, the EC of water in conveyance and drainage canals was measured because the water in these canals represents farm conditions. This measurement was made from the upstream to the downstream regions of the Zeravshan River basin during a field study in August 2017.

First, data from salinity measurements were compared to the spectral reflectance of MODIS bands to determine the bands' sensitivity to EC. Then, 15 salinity and vegetation indices derived from a combination of visible and near-infrared bands were applied to detect soil salinity in this basin.

4.3.1 Zeravshan river basin, Aral Sea Basin

The Zeravshan River basin is the origin of the ancient agricultural and urban civilizations of Central Asia. It is densely populated, especially in the cities, with more than 100,000 people residing in Bukhara, Navoi, and Samarkand (ADB, 2010). Unfortunately, this basin is

heavily impacted by water resource mismanagement because of significant water diversions for irrigation. In addition, a large amount of water is lost due to infiltration into the soil and evaporation (Khujanazarov et al., 2012).

Previously, this basin constituted a subbasin of the Amu Darya River. However, at the turn of the 20th century, this basin was cut off due to increased water diversions for irrigation. As a result, unsustainable water use in this basin is also causing a zone of disconnect in the river flow, with the Zeravshan river retreating upstream due to reduced water flow levels. Fig. 4.3-3 below shows the spatial extent of the Zeravshan river basin in the Aral Sea basin.

Fig. 4.3-3 Zeravshan River basin (ZOï maps, 2016)

4.3.2 Salinity measurements in the Zeravshan river basin

A two-week field study was carried out in the Zeravshan river basin Uzbekistan from July 30th to August 14th, 2017. This study was part of a collaborative investigation with the International Center for Biosaline Agriculture (ICBA). The key objective to measure the spatial gradation of salinity with time along the basin. This investigation formed part of a complementary study to previous observations from 2005 to 2010 by Khujanazarov et al. (2012).

Salinity was measured using a portable EC meter along the Zeravshan river basin. The measurements were taken from transportation and drainage canals that provide and collect water from the farms. These measurements may be justified by a study by Qiu et al. (2017), who found a linear relationship between the EC in irrigation water and the soil in the fields.

4.3.3 Remote sensing indices for salinity assessment in the basin

Soil salinization in this basin occurs mainly due to the secondary salinization of soils. The agricultural irrigation practices here have induced a high accumulation of these toxic salts (Khujanazarov et al., 2012; Toderich et al., 2008). Therefore, 15 salinity indices were applied in this study in an attempt to detect salinized soil. These indices incorporate both direct and indirect salinity detection methods based on the reflectance response of both visible bands (1,3 and 4) and near Infra-Red band 2. The wavelength for these bands is shown in Table 4.3-1 below. In the near infra-red, the spectral response of green leaves is much greater than in any portion of the visible spectrum, while in the visible red band, the reflectance is sensitive to the mesophyll structure of the leaf (CCPO-ODU, 2015).

MOD09GA product which contains the MODIS satellite bands 1 to 7, was used to calculate the vegetation and salinity indices at a spatial resolution of 500m. These indices are shown in Eq. [6-15] in

Table 4.3-2 Salinity detection indices used in this study

	Equation	Applied studies
lex	$RVI = NIR/R$	(Wang et al., 2002
ce Vegetation Index	$NDVI = (NIR - R)/(NIR + R)$	(Wiegand et al., 1
ı Index	$EVI = 2.5(NIR - R)/(NIR + 6R - 7.5BLUE + 1)$	(Lobell et al., 201
ce Salinity Index	$NDSI = (R - NIR)/(R + NIR)$	(Khan et al., 2005
	$BI = \sqrt{(R^2 + NIR^2)}$	(Bouaziz et al., 20
	$SI = \sqrt{Blue \times R}$	(Khan et al., 2005
	$SI1 = \sqrt{G \times R}$	(Bouaziz et al., 20
	$SI2 = \sqrt{G^2 + R^2 + NIR^2}$	(Bouaziz et al., 20
	$SI3 = \sqrt{G^2 + R^2}$	(Bouaziz et al., 20
	$S1 = Blue/R$	(Elhag, 2016)
	$S2 = (Blue - R)/(Blue + R)$	(Elhag, 2016)
	$S3 = (G \times R)/Blue$	(Elhag, 2016)
	$S4 = \sqrt{Blue \times R}$	(Elhag, 2016)
	$S5 = (Blue \times R)/G$	(Elhag, 2016)
	$S6 = (R \times NIR)/G$	(Elhag, 2016)

pg.64.

Since observation by the satellite is at a much coarser scale than the farm size, consideration was made for points appearing in the same satellite pixel. In this case, the EC representing the farm drainage was preferred. Although both the transportation and drainage canals represent conditions on a farm, the drainage canal is assumed to represent the farm's states more accurately.

Table 4.3-1 MODIS visible and near infra-red bands

Band	Wavelength (nm)	Description
1	620-670	Red
2	841-876	Near-InfraRed
3	459-479	Blue
4	545-565	Green

Table 4.3-2 Salinity detection indices used in this study

ndices	Equation	Applied studi
Ratio Vegetation Index	$RVI = NIR/R$	(Wang et al., 2
Normalized Difference Vegetation Index	$NDVI = (NIR - R)/(NIR + R)$	(Wiegand et al
Enhanced Vegetation Index	$EVI = 2.5(NIR - R)/(NIR + 6R - 7.5BLUE + 1)$	(Lobell et al., 2
Normalized Difference Salinity Index	$NDSI = (R - NIR)/(R + NIR)$	(Khan et al., 20
Brightness Index	$BI = \sqrt{(R^2 + NIR^2)}$	(Bouaziz et al.
Salinity Index	$SI = \sqrt{Blue \times R}$	(Khan et al., 20
Salinity Index	$SI1 = \sqrt{G \times R}$	(Bouaziz et al.
Salinity Index	$SI2 = \sqrt{G^2 + R^2 + NIR^2}$	(Bouaziz et al.
Salinity Index	$SI3 = \sqrt{G^2 + R^2}$	(Bouaziz et al.
Salinity Index	$S1 = Blue/R$	(Elhag, 2016)
Salinity Index	$S2 = (Blue - R)/(Blue + R)$	(Elhag, 2016)
Salinity Index	$S3 = (G \times R)/Blue$	(Elhag, 2016)
Salinity Index	$S4 = \sqrt{Blue \times R}$	(Elhag, 2016)
Salinity Index	$S5 = (Blue \times R)/G$	(Elhag, 2016)
Salinity Index	$S6 = (R \times NIR)/G$	(Elhag, 2016)

4.3.4 MODIS bands sensitivity to salinity

The reflectance of these bands at various EC levels varies between Day of Year (DOY) 196 at the start of summer and DOY 273 at the end of summer. These two days were selected due to the presence of cloud-free data from the study site. Summer is an irrigation-intensive period, with the main crop under irrigation being cotton. These two days were also selected since salinity levels continuously increase throughout the irrigation season (Qiu et al., 2017). In this analysis, pronounced sensitivity to salinity varied in the different visible and short wave infra-red bands with no evident trend, as seen in Fig. 4.3-4 below. However, the reflectance was higher at the end of summer than at the beginning of this season. The reasons for which are explained in the subsequent subsections.

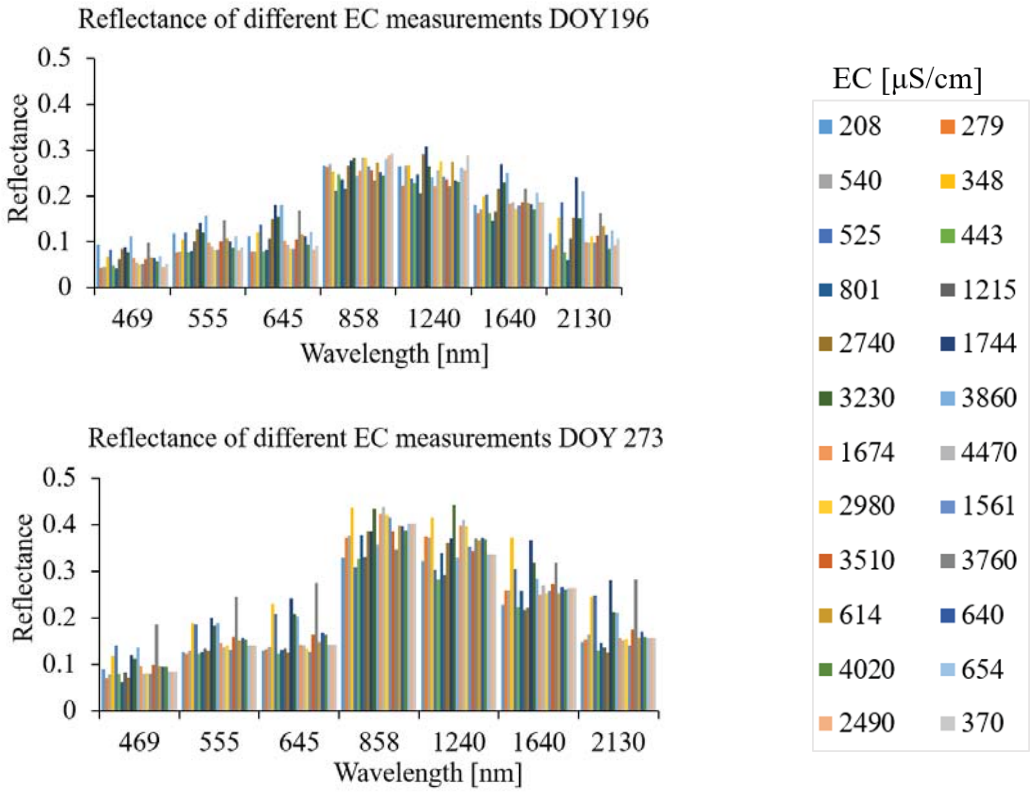

Fig. 4.3-4 Variation of spectral reflectance as a result of the difference in EC; (a) DOY 196 ; (b) DOY 273

4.3.5 Salinity detection by the 15 indices

There was no significant correlation between the vegetation and salinity indices employed and the EC levels measured in the basin. However, the vegetation indices generally decreased with an increase in salinity, while the reflectance indices increased with increasing salinity. An example of this is highlighted here. Fig. 4.3-5 below shows RVI distribution in the Zeravshan River basin. At the beginning of summer (DOY 196), RVI distribution is relatively low, almost evenly distributed in the basin. This low value could be due to the scarcity of vegetation as the crops in the fields are not fully matured. Since RVI is an index detecting vegetation status, DOY 273 is the most ideal for this purpose after crop maturity.

Generally, the RVI correlation with EC was found to have a decreasing trend. This correlation can be seen in (b) below for DOY 273. In the upstream regions of this basin, where salinity was generally lower, the RVI is higher. The converse is valid for the downstream areas of this basin, where the RVI is seen to be lower. Although many factors affect the response of indices detecting the vegetation status, this lowered RVI may be linked to poor plant health due to increased soil salinity. Crops grown in this basin are generally the same, which might trigger the same spectral response from the satellite. However, some farmers switch to more salt-tolerant crop types to adapt to increased soil salinization, which could change the satellite's spectral response.

The correlation coefficient R^2 for all the indices used is shown in Fig. 4.3-6 below (a) to (o) pg.69 Wiegand et al. (1994) found evidence that moisture stress in high osmotic concentration caused by soil salinity induced diminished crop yields. This relation could explain why vegetation indices are reduced with an increase in salinity as plant health is not optimum. Spatial analysis of the gradation of salinity in the whole basin was not very clear both for the vegetation and salinity indices. This unclear trend could be because of the crop

type variability in this basin. Reflectance varies not only due to crop health but is also affected by the crop type. In addition, due to the coarse resolution of MODIS, there are some mixed-cell effects where one mesh contains different crop types, and this influences the retrieved reflectance data. In turn, the results of the computed index are affected

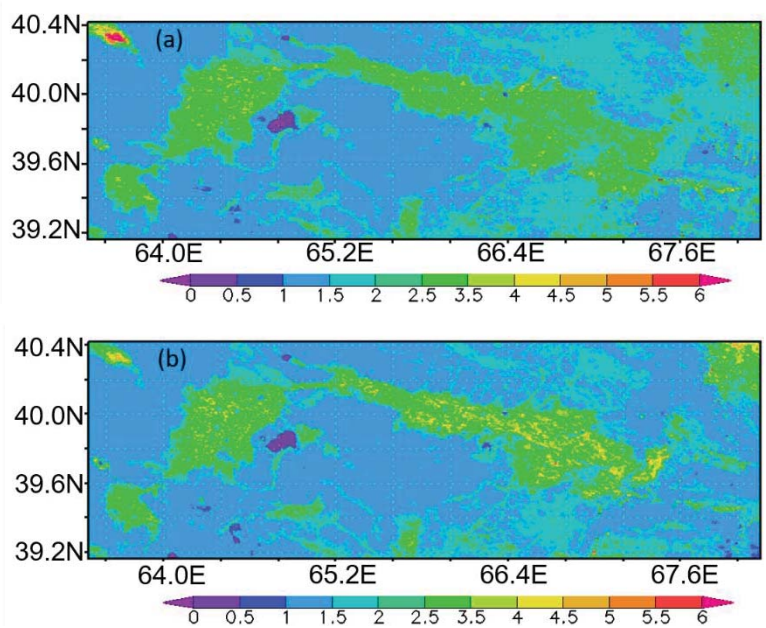

Fig. 4.3-5 RVI distribution in the Zeravshan river basin; (a) DOY 196; (b) DOY 273

4.3.6 Summary

EC collected along the Zeravshan river basin was found to increase from the upstream towards the downstream. However, assessing the sensitivity of the 7 MODIS bands to salinity gradation along the basin revealed no significant correlation between EC and the band reflectance. This lack of correlation may be explained by the fact that reflectance is not only a function of crop health but is also influenced by the basin's diverse crop types.

In general, the vegetation indices decreased with an increase in salinity, while the reflectance indices increased with an increase in salinity. Therefore, although 15 indices were employed

in this study to find the best-suited index for salinity detection, the correlation coefficient R-squared was relatively low.

The highest R-squared value for the indices tested was salinity index SI2 with an R^2 of 0.11. However, since the effects of soil salinization are mainly localized, a basin-scale analysis may be too coarse for the effective detection of salinity. Additionally, at the satellite's resolution, farmlands with many different crop types may be represented by a single pixel. This representation will lead to the mixed-cell effect where the retrieved reflectance data is contaminated by the influence of different crop types and varying crop health.

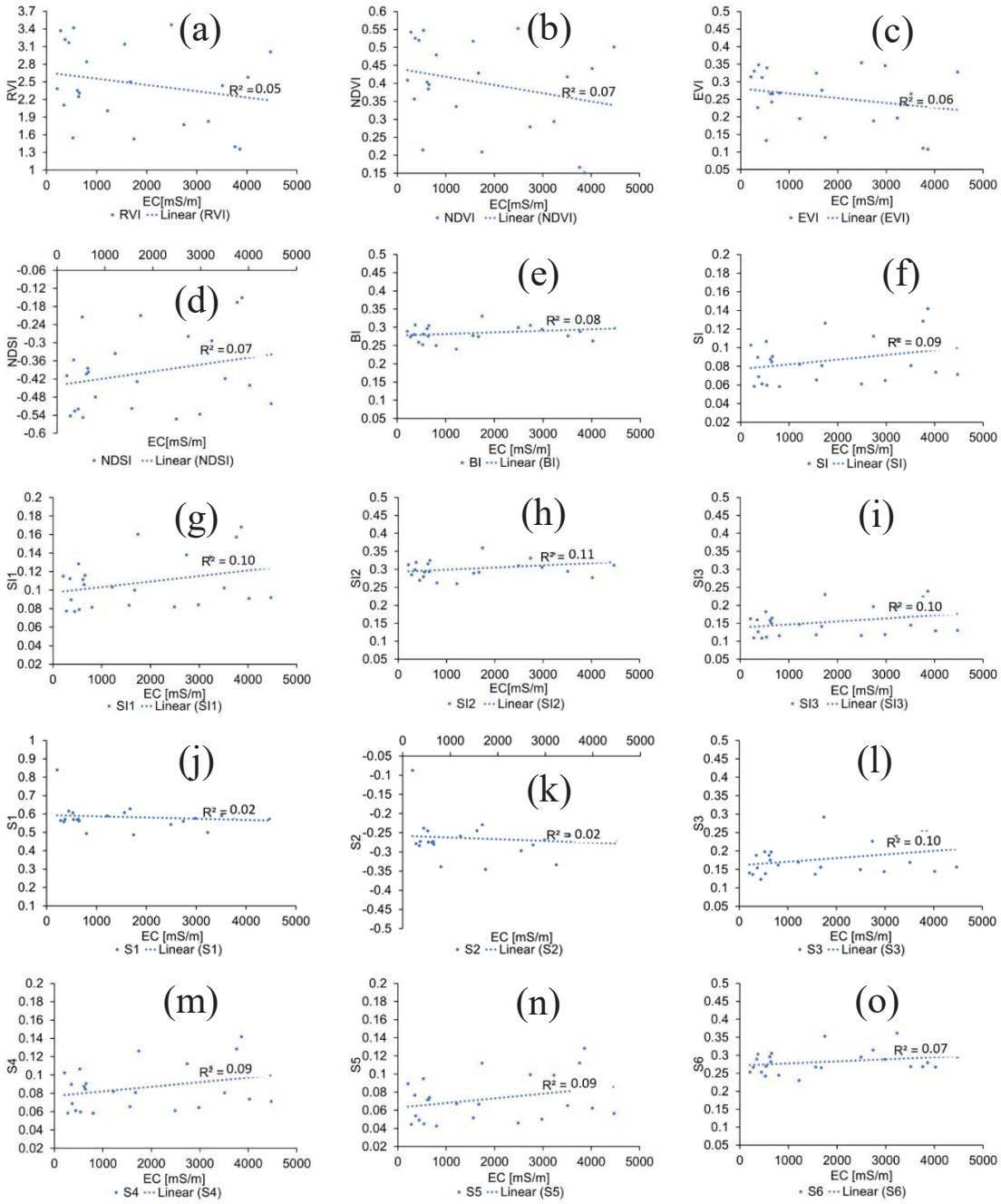

Fig. 4.3-6 Salinity indices used for salinity assessment in the basin; (a) RVI; (b) NDVI; (c) EVI; (d) NDSI; (e) BI; (f) SI; (g) SI 1; (h) SI 2; (i) SI 3; (j) S1; (k) S2; (l) S3; (m) S4; (n) S5; (o) S6

Chapter 5

5 Lake Turkana basin analysis

In this chapter, the SiBUC LSM has been utilized to replicate changes in the basin for the past 18 years. Here, a Lake water balance model is developed, and changes in the basin are validated by considering changes in the Lake's water balance. The reasoning is that all water generated in this basin either evaporates or accumulates in the terminal endorheic Lake. The Lake's storage changes represent changes in the basin's terrestrial water circulation. Additionally, the suitability of the developed model in projecting future changes to the Lake basin is assessed

5.1 Current situation

5.1.1 Background

As discussed in Chapter 2 of this dissertation, the Lake Turkana basin is under increasing pressure from climatic and anthropogenic sources, affecting the basin's water circulation. In order to understand the changes occurring here, a basin-scale hydrological approach is required. Lakes have been reported to act as sentinels of climate change, mimicking any modifications instigated in their basins (Adrian et al., 2009). Therefore, changes in the basin, whether anthropogenic or climatic, can be identified through changes in the Lake's water storage. Additionally, one of the impacts of climate change on Lakes has been determined to be a 50 percent retention of temperatures gained in the upper layer (Verburg et al., 2003). Subsequently, this increase in temperature would result in increased evaporation, which would increase the salinity, the consequences of which are discussed in Chapter 2.

Although the hydrological components in this basin impact the Lake's existence, they are still understudied and therefore not well understood. Nevertheless, some studies have been carried out to assess the impact of the damming of the Omo River and the increase

of irrigated area on the Lake (Avery, 2012b, 2010; Avery and Tebbs, 2018; Spruill, 2019; UNEP, 2013; Velpuri et al., 2012). In Avery (2010), (2012b), and Avery and Tebbs (2018), a water balance model was developed to estimate the change of storage in the Lake. However, this model was centered on the Lake itself, considering the precipitation and evaporative losses but did not consider other parameters, which affect water availability in the basin. The other studies employed a basin-scale approach. Spruill (2019) used satellite-derived datasets to calculate the change in storage. However, irrigation influences and base flow were not considered. The lake storage shifts were estimated from the basin-scale difference between soil moisture changes and evaporation from the total basin precipitation. In UNEP (2013), and Velpuri et al. (2012), the Lake Level Modelling (LLM) approach was used to estimate the Lake's water levels. Here, runoff, including surface and base flow, was calculated based on the Vegetation ET (VegET) model, which conducts operational vegetation water balances of rainfed systems (Senay, 2008). Although the LLM approach favorably replicated long-term trends in the lake level variations, the influence of irrigation water was not considered.

In these previous studies, methods to replicate changes in the water balance were developed. The reasons for these changes, on the other hand, were not adequately explained. Furthermore, the effect of irrigation, which is of increasing concern in the basin, was not taken into account. Therefore, in this study, we aim to develop a method that can be used to estimate the sustainability in endorheic basins by considering terrestrial water circulation. Here, a lake model was developed coupled with the SiBUC LSM. This method can consider the effect of irrigation and climate change. It's challenging to replicate variations in a lake's water balance in the face of climate change and anthropogenic influences. However, since this study is based on a basin-scale approach for water balance consideration, any climatic and anthropogenic impacts in the basin can be evaluated through their influence on the Lake's resultant influx.

Therefore, the main objectives of this study are (i) to develop a water balance model coupled with the SiBUC LSM to reproduce changes to Lake Turkana water storage considering the influence of irrigation, (ii) to explain the changes in the Lake's water storage by considering changes in hydrological components in the basin. This method will provide a robust platform to estimate future changes to the Lake's water storage. Here, climate change and the growing water demand from irrigation can be considered. The SiBUC LSM has been applied successfully in Central Asia, where irrigation was of significant consequence to the desiccation of the Aral Sea (Touge et al., 2013).

5.1.2 Methodology development

In this study, basin-scale numerical simulation considering the effect of irrigation was analyzed to understand the basin-scale heat and water balance cycles. First, the runoff generated by each mesh in the basin was calculated. This runoff was then used to estimate inflow to the Lake from the basin. Finally, the Lake's water balance was calculated. All the computations here are in millimeters(mm). The mesh runoff is described in Eq.(19) below.

$$Q = P - E - dSm \tag{19}$$

where Q is the mesh runoff, including the surface and base flow, P is the precipitation, E is the evapotranspiration, and dSm is the change in soil moisture. Inflow to the lake from the basin was calculated as shown in Eq.(20) below.

$$Q_{in} = \sum Q - \sum \frac{win}{\gamma} - \sum wout \tag{20}$$

where Q_{in} is the inflow to the Lake, ΣQ is the summation of runoff from all the meshes, $\sum \frac{win}{\gamma}$ is the summation of all the irrigation water requirement considering the water conveyance efficiency γ, and $\sum wout$ is the summation of drainage water from all the meshes. Water consumed outside the basin, which cannot be physically considered using

a vertical 1-dimension analysis, was omitted in Eq.(20) above. Finally, the water balance in the Lake was calculated using Eq.(21) below.

$$dS_{Turk} = Q_{in} + (P - E)_{Turk} \tag{21}$$

where *dS* is the change in storage, and the subscript *Turk* represents calculations for the Lake Turkana.

5.1.3 Preparation of model input data

The SiBUC LSM was used to run hourly numerical simulations for 18 years, from 2001 to 2018, at a spatial resolution of 5 km. First, MERIT hydro flow direction data was used to delineate the boundaries of the Lake Turkana basin by determining the flow direction from each cell to its steepest downslope neighbor. After that, the basin meshes were upscaled to a resolution of 5 kilometers. Next, the Inverse Distance Weighting (IDW) method was used to downscale meteorological forcing data to this resolution, and hourly data were linearly interpolated.

For the consideration of the irrigation area, the ESA LC product was applied. However, because this product's irrigation class includes post-flooding, the Global Map of Irrigation fraction was used to isolate the expanse of the irrigation land. Subsequently, the area under irrigation was calculated and compared to actual basin irrigation area statistics, provided by Frenken (2005) for the Omo-Gibe basin and Maina et al. (2013) for the Turkwel and Kerio basins.

Table 5.1-1 Summary of the irrigated area data sources

Data	Period	Data source	Data scale
ESA Land Cover	1992 to 2019	Satellite	Global 300m ×300m
Global Map of Irrigation fraction	2005	Irrigation statistics and Geospatial data	Global 5 arcmin×5 arcmin
Frenken (2005)	2001		Omo-Gibe Basin
Maina et al. (2013)	Not mentioned	Statistics	Turkwel and Kerio Basins

The total area irrigated by the ESA LC was underestimated, but it grew steadily during the study period. As such, first, the meshes that were thought to be irrigated were identified. Then the irrigation area in basin sectors with a concentration of irrigation land, as presented by Awulachew et al. (2007), was expanded. However, since the irrigation area statistic was for 2001, a rate of expansion for the irrigated area given by the ESA LC trend was assumed. Finally, the land uses of the other classes were reduced proportionately to accommodate the expanding irrigation land Fig. 5.1-1 pg75. A summary of the irrigated area data is shown in Table 5.1-1 above.

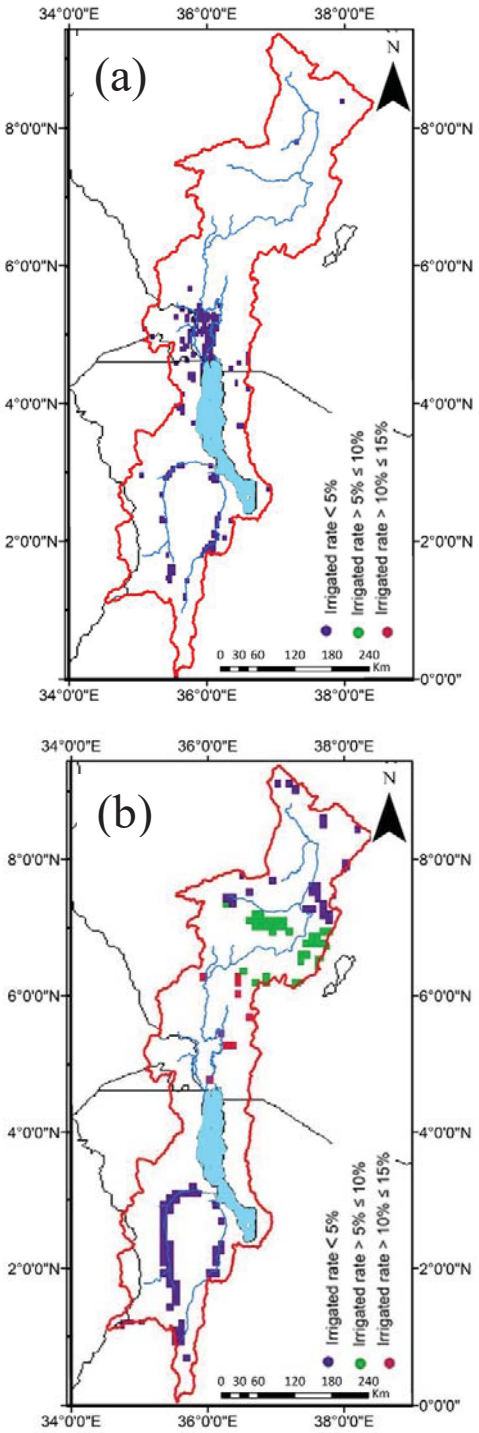

Fig. 5.1-1 Modification of the ESA LC irrigated area; (a) original irrigated area, which includes post-flooding; (b) the final irrigated area with expansion in the irrigation intensive zones

5.1.4 The endorheic lake water balance model

The advantages of this model are that the dynamic shifts in the lake levels, albeit small, can be considered, and the subsequent change in land use can be reflected in the SiBUC LSM. The lakebed was smoothed to improve the model's accuracy and improve the gradation of elevation with depth. For this purpose, SRTM DEM and bathymetry data with a resolution of 90m were used. First, the elevation of the lakebed was obtained by subtracting the lake bathymetry from the SRTM DEM which provides the surface elevation of the Lake. Then since the lake level has been noted to fluctuate between the elevations of 350m to 366m (Velpuri et al., 2012), the elevation of the lake bed between these two levels was linearly interpolated.

The relationship between the Lake area and the interpolated elevation can be seen in Fig. 5.1-2 pg.77. As the lake level increases, more meshes surrounding the Lake become inundated, resulting in an increase in the Lake area. The converse is true for a reduction in the Lake level. When the lake level reduces, meshes on the Lake's edges dry up, decreasing the subsequent lake area. This relationship between the lake level changes and the lake area is critical to consider as it affects the heat fluxes on the Lake. A larger surface area would translate into higher evaporative rates as more of the Lake's surface becomes heated by radiation. This relationship between the elevation and the lake area shows a similar trend as that reported in previous studies (See Fig. 5.1-2 (b) pg.77).

The gradation of elevation in the Lake is comparable to the altimeter satellite depiction of elevation here (See Fig. 5.1-3 pg.77). As mentioned in chapter 3, the inflow is used as a determiner for the lake level by this model. More about the replication of the Lake inflow is discussed in the subsequent sections.

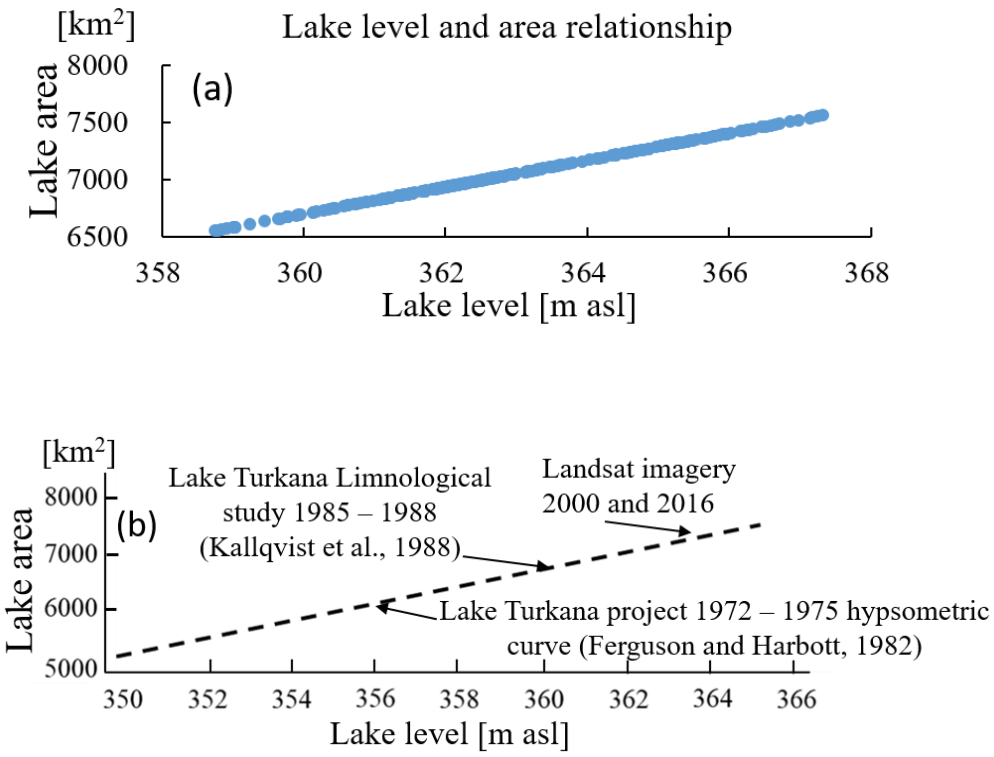

Fig. 5.1-2 Relationship between the lake area and level; (a) Interpolated Lake level and area relationship; (b) Lake area and level relationship from previous studies (Avery and Tebbs, 2018b)

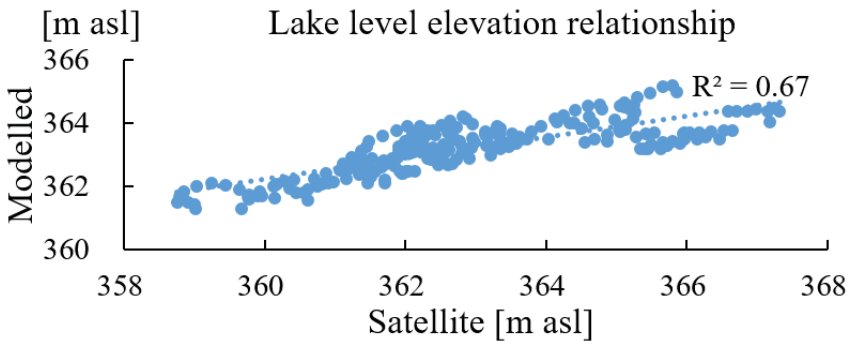

Fig. 5.1-3 Correlation between modeled and Satellite lake level

5.1.5 Reproducing change the Lake Turkana level

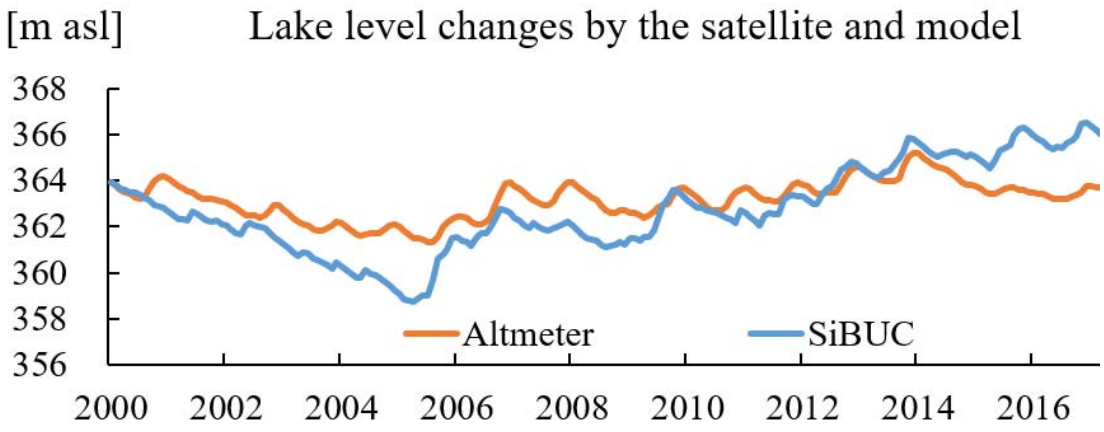

Fig. 5.1-4 Modeled and satellite depicted lake level changes from 2001 to 2018

As mentioned in the objectives, the numerically analyzed changes in the water level of Lake Turkana are presented here. In the absence of inflow data, the model efficacy was evaluated by comparing changes in the physically analyzed storage to that assessed by the altimetry satellite. However, it is imperative to note that using such information as a validation tool has limitations, particularly since Lake Turkana is subjected to strong winds daily. Wind and tidal changes may affect the accuracy of the altimetry data (Avery, 2010; USDA, 2016). However, the wind's bearing on the Lake is described as stretching northwest, while the satellite altimetry direction is near the Lake's center. Therefore, satellite altimetry is supposed to be indicative of the Lake's conditions (Avery, 2010).

Fig. 5.1-4 pg.78 illustrates the relationship between the physically analyzed and altimeter satellite-depicted changes in the lake level. The results show that the suggested methodology could replicate the Lake's seasonal fluctuations from 2001 to 2018. In addition, the rise in the lake level from 2006 to 2007 and the subsequent decreases in 2008 to 2010, 2011 to 2012, and 2016 could be captured. The altimeter satellite and model analyzed lake level changes also show a relatively strong correlation with a Pearson's coefficient (r) of 0.82.

However, it was noted that the analyzed inflow to the Lake was underestimated during dry years and overestimated during wet years, presenting the disparity between the analyzed lake level and the altimeter satellite depicted lake level changes. This could be a result of uncertainties introduced by various factors during the simulation, including the input data or parameterization by the model.

Despite this, since the focus of this study is to estimate and explain the lake level changes considering the irrigation effect, the model results are sufficient for this purpose. Therefore, the explanation for the lake level changes can be described by examining changes occurring in this basin. Accordingly, since our approach takes irrigation water requirements into account, the model can be sufficiently accurate in predicting possible changes in the basin by integrating future climate data and considering the anticipated changes in land use.

5.1.6 Understanding the water balance components in the Lake Turkana Basin

Understanding the hydrological components in this basin is required to clarify changes in the Lake's water storage. First, the physical components used in the water balance equations (19) - (21) were spatially analyzed. This spatial analysis provides an understanding of the main driving factors for storage changes in this Lake. Fig. 5.1-5 pg.81 shows an 18-year average of these components at a spatial resolution of 5km. As precipitation is the main driving force for any water balance assessment, its distribution in the basin is evaluated first. Rainfall was found to be three times higher in the high elevation regions at the basin's northern and southern ends and lowest in the low elevation regions near the Lake (See Fig. 5.1-5 a).

Consequently, soil moisture followed the same trend. The regions at higher elevations had a moisture content two times greater than those at lower elevations (See Fig. 5.1-5 b). Although soil moisture is a function of many variables, including soil type and land use, Sehler et al. (2019) reported a strong correlation between precipitation and soil moisture

in arid regions. The differences in rainfall and soil moisture allow for a better understanding of the evaporative losses in the basin, which shape the runoff.

Radiation is the primary source of energy influencing fluxes in this basin. It strongly impacts the basin's evaporative losses. In the lower elevation regions close to the Lake, the radiation temperature was between 5 to 10 °C higher than in the high elevation regions (See Fig. 5.1-5 c).

The analyzed runoff understandably demonstrated the high evaporative losses in this basin (See Fig. 5.1-5 d). Although more than 1000mm of rainfall was received in the high elevation regions, only about 300mm of runoff was generated (See Fig. 5.1-5 e). This figure indicates that more than 70 percent of moisture in this basin is lost through evaporation.

Subsequently, the precipitation and evaporative rates of the Lake were analyzed to assess the main factors contributing to water storage changes. The evaporation rates from the Lake's surface were found to be significantly higher than the precipitation received. Actually, by evaporation, nine times more water than rainfall is lost. Since this is a closed lake with no outflow and minor seepage (Ricketts and Johnson, 1996), runoff generating inflow into the Lake is an essential sensitive water store indicator. Therefore, the Lake's water levels will be affected by any changes in the basin, either climatic or anthropogenic, which affect water availability.

As such, irrigation is an essential factor to consider because it derives from the runoff. In the intensive agricultural areas of the basin, the analyzed irrigation water requirement is approximately 400mm (See Fig. 5.1-5 e). This water requirement is similar compared to Yimer (2018) study. Conversely, if the irrigation area in this basin is expanded, more water will be withdrawn, reducing the lake's crucial inflow that replaces the evaporated water.

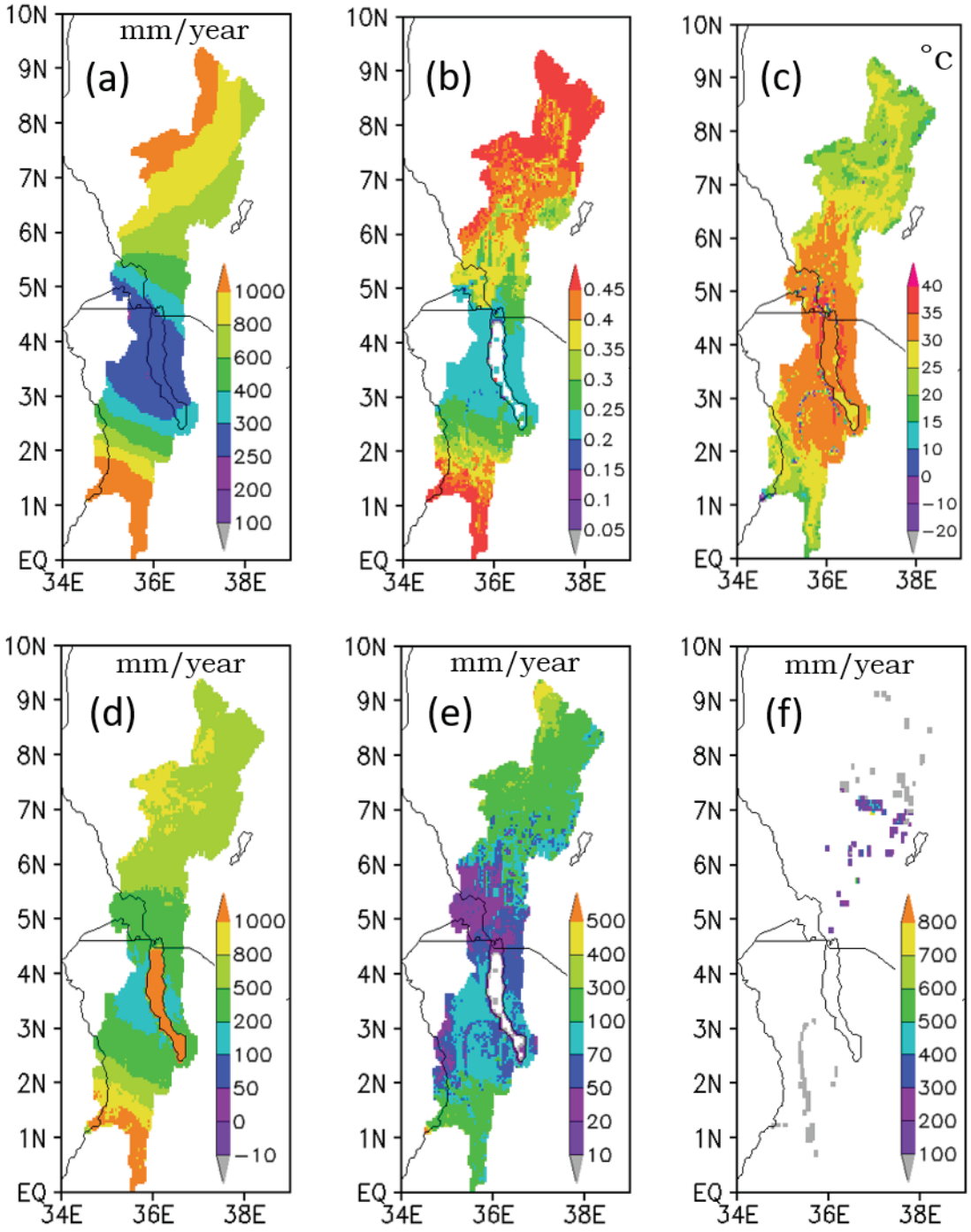

Fig. 5.1-5 18-year averaged distribution of analyzed parameters at a 5km spatial resolution; (a) Rainfall; (b)Soil moisture; (c) Temperature (d) Evapotranspiration; (e) Runoff; (f) Irrigated area

5.1.7 Reason for the changes in the lake level

The main objective is to explain the reason for the changes in the lake level by observing the changes in the hydrological components in this basin. The notable variations in the lake level in 2006, its decrease in 2009, 2010, 2012, and 2016 are discussed. Additionally, the increasing trend in the lake level is also clarified.

First, observation of rainfall which is the primary water source, and temperature, which is the main energy source in this basin affecting heat fluxes, sheds light on the reasons for some of these variations. Fig. 5.1-6 pg.84 shows the changes in the total monthly rainfall and average monthly temperatures in this basin from 2001 to 2018. While Fig. 5.1-7 pg.84 shows the variations of the monthly Lake inflow (Qin) and the average monthly temperatures in the basin for the same period.

At the beginning of the decade, the basin suffered decreased rainfall while the average temperatures were higher by approximately 0.4°C. This increase in the average temperature and the total monthly rainfall reduction led to a decrease in the lake level. As a result, the East African region reportedly suffered a prevailing drought with a shortage of rainfall during this period, with some areas receiving only 50 percent of the expected precipitation (Adrian et al., 2009; Nicholson, 2014).

The steep increase in the lake levels towards the end of 2006 and 2007 may be attributed to the increase in rainfall and decreased average temperature for the same period. Here, the precipitation increased by more than 50 percent of the level received in 2005. Rainfall in the Ethiopian highlands was markedly higher than average in the second half of 2006 and 2007, with flooding reported in some parts of the country (Jury, 2011). Additionally, the heavy rainfall was said to have triggered the peak runoff in the Gibe River during this period (Woldegebrael et al., 2020).

Towards the end of 2009 to 2010, the lake level slightly decreased again. This reduction in the lake level can also be attributed to increased temperatures with an accompanying

decrease in rainfall. During this period, the average temperature in the basin rose by 0.2°C compared to 2008, while precipitation decreased by around 5 percent. As a result, a famine was recorded in East Africa due to prevailing dry conditions caused by below-average rainfall (Nicholson, 2014).

A similar drought was suffered in this basin from 2011 to 2012. During this period, the temperatures increased by 0.2^{o}C of the level in 2009 while the rainfall reduced by about 4 percent. As a result, 2011 was hailed as one of the driest years in the region with below-average precipitation (OCHA, 2011).

The lake level continued to rise steadily until mid-2015 to 2016, where it dropped again. During this period, a severe drought related to La Niña was reported in this basin (OCHA, 2011). Additionally, the Gibe III dam was inaugurated and started filling (Salini Impregilo, 2016). Temperatures increased by approximately 0.2^{o}C compared to the 2014 levels during this period, while rainfall decreased slightly by about 2 percent.

As seen from the above narratives, Lake Turkana water levels are easily affected by climatic changes in this basin. The frequent droughts caused periodic drops in the lake level. Generally, at the beginning of the decade until 2006, the average temperatures in this basin were approximately 27.5^{o}C. However, the average temperature in this basin decreased by about 0.2℃ from 2006 to 2018.

The opposite effect occurred for the rainfall. From the beginning of the decade until 2006, the average precipitation in this basin was approximately 560mm per year. However, from 2006 to 2018, the yearly rainfall in this basin increased by roughly 30 percent.

As a result, climate change in this basin may be a factor influencing the changing lake levels. While several factors, such as changes in the lake bed and the basin's water

demand, may be contributing to the increasing lake level, climate change may also be an influencing factor.

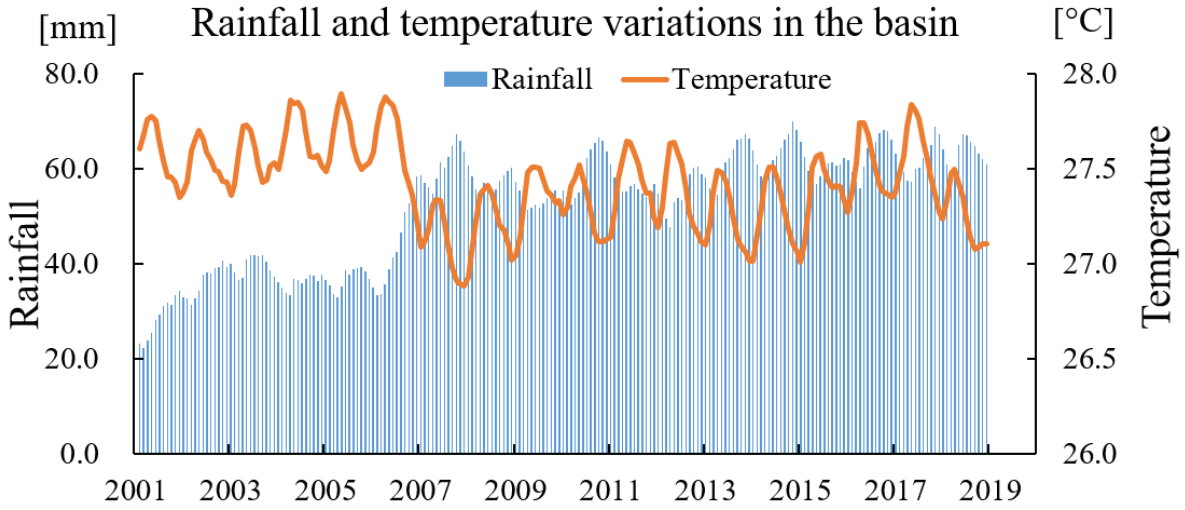

Fig. 5.1-6 Monthy Rainfall and Temperature variations in this basin from 2001 to 2018

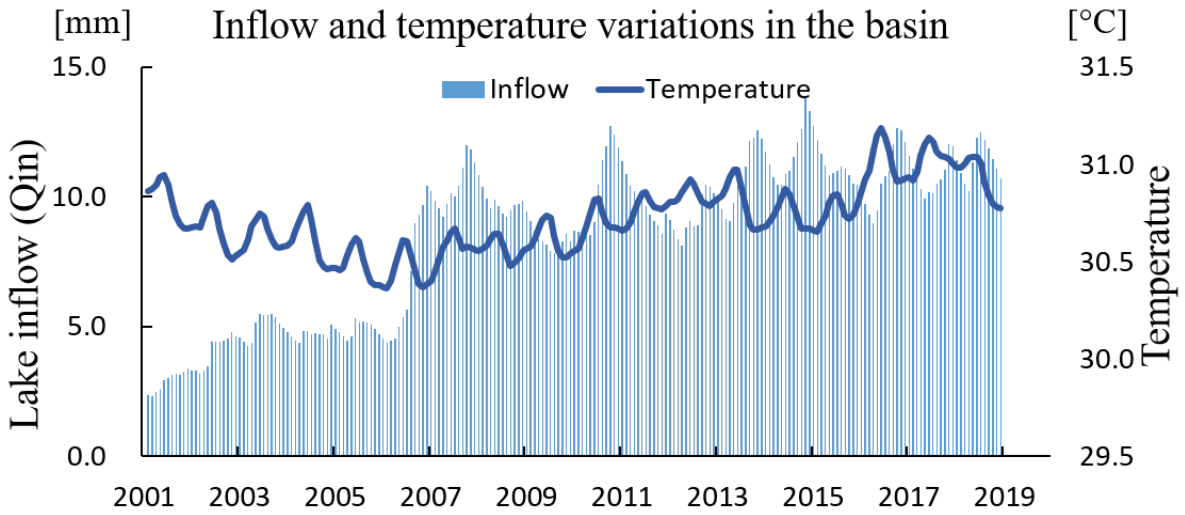

Fig. 5.1-7 The relationship between lake inflow and temperature variations in this basin

5.1.8 Changes in the basin water balance

The water balance components in this basin have experienced changes, as observed from this assessment. To illustrate this, the analysis period was divided into six bands of three years each. This evaluation demonstrates the abrupt changes in the terrestrial water circulation here.

First, rainfall, which is the most important factor affecting water supply, increased steadily from 2001 to 2018. Since the Lake is in an arid zone, however, precipitation did not change as much here. As a result, the difference between lake precipitation and evaporation has remained relatively constant.

Furthermore, the increased inflow to the Lake can be attributed to this increase in the basin's average rainfall. Towards the end of the second decade, the inflow (Qin) increased by more than 100 percent.

Ordinarily, this increased rainfall has also contributed to a surge in the basin's evaporative rates. Concurrently, rainfall is the primary driver in this basin, influencing changes in the lake water balance. See **Table 5.1-2** below.

Table 5.1-2 Water balance changes in the basin

Years	Rainfall [mm/year]	Evaporation [mm/year]	Inflow(Qin) [mm/year]	Lake Rain-Evap [mm/year]
2001-2003	514	461	66	-1892
2004-2006	626	497	105	-1727
2007-2009	684	596	109	-1907
2010-2012	715	592	130	-1787
2013-2015	787	650	142	-1989
2016-2018	758	637	138	-1987

5.2 Future changes to the Lake water balance

BCC-CSM2-MR from the Beijing Climate Center China is used to assess the suitability of the developed model in estimating future changes to the lake water balance. This model has a spatial resolution of 100km with the meteorological forcing variables at 6 and 3 hours. The data was downscaled using the IDW method, and the temporal data were linearly interpolated to hourly.

5.2.1 Background

As mentioned in chapter 2, the Lake Turkana basin is rapidly changing. Due to the rising population, erratic precipitation patterns, the desire to increase crop production, and the means for financial resources to implement projects, the irrigation areas in this basin have been growing.

Numerous irrigation area expansion plans have already been tabled. These include; establishing a 1000km^2 sugarcane irrigation scheme as part of a 15-year project scheduled to conclude in 2026 (Government of Ethiopia, 2018). However, only 106km^2 of the planned 1000km^2 excision has been cultivated, with an additional 130km^2 cleared but not cultivated (Kamski, 2016). Additionally, there are plans to increase cotton land allocation by approximately 400 km^2 (ibid.). In Kenya, plans call for the establishment of a 300 km^2 irrigation scheme in the Turkwel river's lower reaches (Ondimu et al., 2018). Furthermore, a 100 km^2 irrigation scheme will be established at Todenyang, near Lake Turkana (Avery and Tebbs, 2018a). The irrigated area potential in the Omo River basin, the primary water source for the Lake, is estimated as between 700km^2 to 4450km^2, depending on the source (Awulachew et al., 2007).

Therefore, increased water abstraction to meet the growing needs for irrigation is expected. When this occurs, lake levels will begin to decline, and an environmental disaster on the scale of the Aral Sea Basin will become unavoidable.

5.2.2 Irrigation scenario

The irrigation scenarios are categorized into three, depending on the likelihood of project completion. Hence, in scenario 1, the expected changes are based on the full implementation of irrigation on the currently excised land. This scenario includes the full irrigation of the 130km^2 cleared for sugarcane plantations and the development of the Todenyang irrigation scheme in Kenya.

Table 5.2-1 Irrigation scenarios established

Scenario	Status	Irrigation area [km^2]	Literature review
1	Current + Scenario1	660	(Frenken, 2012; Kamski, 2016; Maina et al., 2013)
2	Current + Scenario2	1488	(Avery, 2012a; Government of Ethiopia, 2018; Ondimu et al., 2018)
3	60 percent of the irrigation potential	1800	(Avery, 2012a; Awulachew et al., 2007)

Then the second scenario is based on the implementation of 80 percent of the current ongoing projects. Since the current projects are already delayed, this scenario will assume an 80 percent likely hood of completing the envisaged projects during this timeframe. For this, the 1000km^2 sugarcane irrigation project, the 300km^2 irrigation scheme set to be established in Kenya, and the 400km^2 expansion of land for cotton irrigation will be considered. Finally, the last scenario is based on the full implementation of all the ongoing projects. With this, approximately 60 percent of the basin's total irrigated area potential will be consumed. Table 5.2-1 above shows a summary of the irrigation scenarios developed for this study.

5.2.3 Downscaling and bias correction

The GCM model used, BCC-CSM2-MR SSP585 from the Beijing Climate Center, was downscaled using the inverse distance weighting method, and the temporal data were linearly interpolated. The data was downscaled to 5km spatial resolution and hourly data output.

This model provides meteorological forcing at a spatial resolution of 100km. The meteorological forcing variables specific humidity, air temperature, and wind at 6 hours and surface air pressure, precipitation, and surface downwelling longwave and short wave at 3 hours.

The model data was bias-corrected using the delta method since all the seven variables required for numerical simulation are of significant importance influencing the model output.

5.2.4 Irrigation water demand and Inflow changes

The irrigation water demand in the three scenarios also impacts the resultant inflow to the lake (See Fig. 5.2-1). As the irrigation area increases, the total water demand in the basin increases, leading to a decrease in the consequent inflow to the lake.

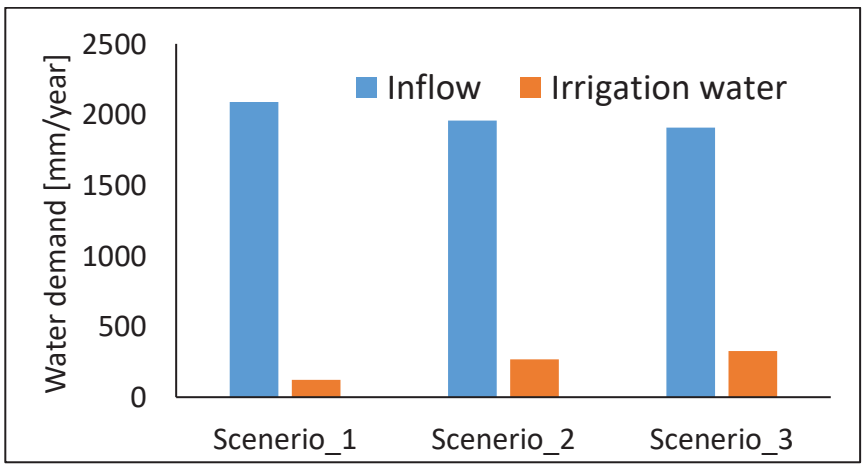

Fig. 5.2-1 Inflow and irrigation water requirement for 3 furute scenerios

5.3 Summary

In this study, the main objective was to develop an endorheic lake water balance model to predict future changes in this basin considering irrigated areas. Additionally, this study aimed to explain the Lake's water balance changes through a basin-scale analysis of the hydrological components.

The developed water balance model displayed sensitivity in identifying the relationship between changes in the Lake's water level and area. This relationship is essential as it affects heat fluxes on the Lake's surface and determines the evaporative rates of the Lake.

In the absence of statistical Lake level validation data, the altimeter satellite was employed. First, the gradation of elevation in the Lake was compared. Although the absolute value of the lake level was different, the relationship between the analyzed Lake level and the satellite depicted lake level changes showed a linear trend. This relationship illustrates the ability of the developed model to capture the changes in the Lake level accurately.

Moreover, the precipitation and radiative temperatures play a vital role in the availability of water in this basin. More than 70 percent of water here is lost through evaporation.

When comparing the analyzed changes in the lake level from 2001 to 2018 to the satellite depicted changes, a similar trend is ascertained. Here, the analyzed changes in the lake level can adequately detect the seasonal variations in this Lake with a correlation R^2 of 0.82.

Additionally, the changes in the lake level can be linked to changes in the temperature and precipitation here. Generally, the temperatures here have decreased by about 0.2^oC, with the rainfall increasing by about 30 percent.

Chapter 6

6 Endorheic lakes sustainability assessment

This chapter assesses the threshold for sustainable changes in endorheic basins based on the volume and surface area variance. The changes in the Aral Sea are evaluated against those occurring in the Lake Turkana Basin. Conclusions in this chapter are based on the different instigated changes as observed in the endorheic Lake basins.

6.1 Background

Global endorheic lakes are sensitive to changes in terrestrial water circulation. Broadly speaking, these lakes may be categorized into three; (i) Stable lakes with no long-term changes in water storage, (ii) Lakes in danger of shrinking due to increasing anthropogenic influences in the basin, exacerbated by climate change, and (iii) Severely desiccated Lakes. In this dissertation, various methodologies were explored to assess changes in the Aral Sea in Central Asia and Lake Turkana in Eastern Africa.

These water bodies are found in endorheic basins located in arid and semi-arid environments. Since the Aral Sea is already severely depleted, it is considered a changed endorheic lake in category (iii). On the other hand, Lake Turkana is regarded as a changing lake in category (ii) due to increased anthropogenic activities in the basin, which may jeopardize the Lake's existence.

As discussed in chapters two, four, and five, the lake volume and area changes have been attributed to severe consequences. Moreover, phenomena of extreme water fluctuations are significant in endorheic lakes worldwide. Due to the small ratio of water volume storage to annual inflow in an endorheic lake, changes in basin-scale water balance easily affect these lakes'.

Therefore, an integrated assessment of Lakes under different statuses can propagate a better understanding of sustainability by comparing the variation of volume and area and

the resultant environmental impact. The changing trend and standard deviation of the volume and area in the Aral Sea and Lake Turkana were assessed. For the Aral Sea, past changes from 1960 to 2000 were evaluated. While the changes in the trend of the current situation and future situation were assessed for Lake Turkana. Here the GCM BCC-CSM2-MR from the Beijing Climate Center China is used with the SSP585. The irrigation scenarios 1,2 and 3 were employed

6.2 Trend and variation in volume sustainability assessment

The Aral Sea changes in volume trend and the standard deviation for each decade from 1960 to 2000 were analyzed. Additionally, the volume and standard deviation for Lake Turkana's current and future changes were also analyzed. The results for these two endorheic basins were then assessed to establish the sustainability threshold in endorheic lakes.

Fig. 6.2-1 below shows the sustainability of endorheic lakes based on volume assessment in the Aral Sea and Lake Turkana. The more stable the lake, the closer the point is to zero. Additionally, the plotted points for an expanding lake would shift to the right due to a positive increase in the trend. On the other hand, a shrinking lake would shift to the left due to a decrease in trend. The difference of trend and standard deviation changes between irrigation scenarios 1,2,3 are too small to be isolated.

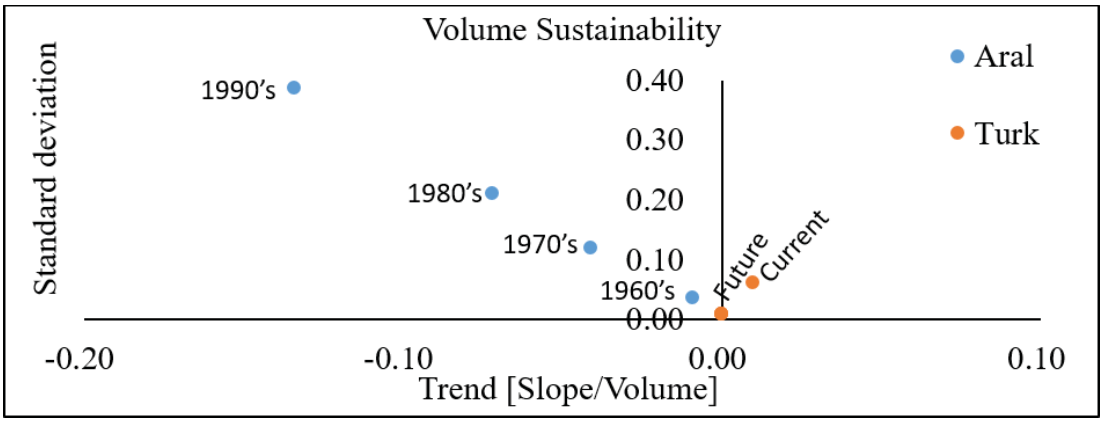

Fig. 6.2-1 Volume changes in the Aral Sea and Lake Turkana

The plotted points on the left side of the y-axis illustrate the variability in the Aral Sea basin leading up to 2000. As the Sea continued to shrink, the volume decreased. By the 1970s, the effects of the shrinking lake on the environment were imminent. The fishing industry was experiencing a steady decrease in harvest, while the salinity in the Sea was on a steady rise. Since the fishing industry is highly susceptible to salinity changes, this decade experienced the most significant and rapid loss in fish harvest, driving the industry to an almost total collapse. Finally, in the 1980s, a complete failure of the fishing industry occurred. At this time, the salinity levels increased way above 20g/l as the volume in the Sea decreased by nearly a half. By the end of the 1990s, the volume of the Sea was about 10 percent of the initial volume in 1960.

In Lake Turkana, the changes in the lake volume are not as severe as that of the Aral Sea. Therefore, although the trend in the current analysis expressed a positive increase in the volume, the variance in this was not quite as significant. In fact, this current trend is almost similar to the trend in the Aral Sea in the 1960s. However, in the future analysis (end of the century), the lake experiences a decreasing trend in volume. Generally, the standard deviation in the volume is expected to be more prominent in the future, but the changes are not likely to be significant. However, the variance here is relatively small, indicating a state of stability in the Lake's volume. This future assessment is simulated

assuming a progressive increase in the irrigated area in scenarios 1, 2, and 3 in the basin, with the climatic scenario SSP585.

6.3 Trend and variation in area sustainability assessment

An assessment of the area changes for both lakes for the same period mentioned above highlights the difference in area sustainability for inland lakes (See Fig. 6.3-1 below). Just like the volume, The more stable the lake, the closer the point is to zero. Additionally, the plotted points for an expanding lake would shift to the right due to a positive increase in the trend, while a shrinking lake would shift to the left due to a decrease in trend.

In this figure, the plotted points on the left side of the y-axis illustrate the variability in the Aral Sea basin leading up to 2000. As the Sea continued to shrink, the area decreased, and the standard deviation of the area also increased. In the 1960s, the area of the Aral Sea began to diminish. By the 1970s and 1980s, the Sea area had reduced by nearly half, and effects of this were already being suffered. Although the Sea continued to shrink during this period steadily, variance in the area was not quite as significant as that of the volume. During this period, a study in a province downstream of the Aral Sea basin reported a correlation between respiratory diseases and the reducing lake area. Around 60 percent of children under the age of one who perished here died of respiratory infections, and 97 percent of these fatalities were from acute pneumonia (Glantz, 1999). Additionally, it was revealed that about 45.6 percent of children residing in this area were also ill. By 2000, the Sea area had decreased to about 10 percent of its previous level in 1960.

Much like variability in the volume, changes in the area in Lake Turkana were not quite as severe as that of the Aral Sea. However, the trend in the current analysis also expressed a positive increase in the area, with the future analysis showing a decreasing trend of the same. This trend in the current analysis is also almost similar to the trend in the Aral Sea in the 1960s. However, in future analysis, the variance in the area is still relatively small in all irrigation scenarios, indicating a state of stability in the Lake’s area.

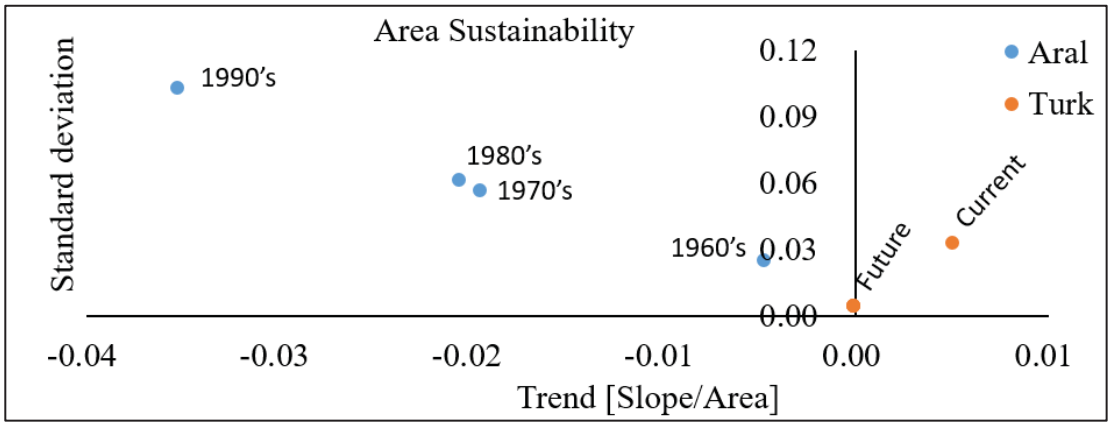

Fig. 6.3-1 Area changes in the Aral Sea and Lake Turkana

6.4 Summary

From the above discussions, it can be elucidated that examining the variation of both volume and area in an endorheic lake can provide some understanding of the status of the Lake. The larger the changes in the trend, the more significant the impact of water balance changes on the surrounding environment. Additionally, examining the changes in the variation of both area and volume can provide an understanding of the extent of short-term changes in the lake.

In this case, a stable lake would exhibit minor changes in the variation of the trend and standard deviation with the plotted point of the same approaching zero. In contrast, a rapidly changing lake will experience a more considerable variation in volume and area changes. Therefore, the sustainability of global inland lakes can be assessed by comparing lakes of different sustainability clusters to evaluate the long-term changes occurring in the lakes' water balance.

Chapter 7

7 Conclusions and Recommendations

7.1 Conclusions

This dissertation aimed to develop methodologies to assess irrigation influences on hydrological components in endorheic basins, taking climate change into account. This aim was proliferated by the recent changes in global endorheic basins, which are altering the heat and water balance cycles here. To this effect, the following five objectives were developed. First, to identify changes occurring in endorheic basins by comparing Lake Turkana to the Aral Sea. Second, to improve the detection of irrigation areas using the land surface model's analyzed radiative temperature and satellite-based land surface temperature. Third, to assess the spatial and temporal distribution of irrigation-induced salinity in endorheic basins. Fourth, to explain changes in the water balance of endorheic lakes by developing a storage change model integrated with a land surface model. Lastly, to assess sustainability in endorheic lakes by considering long-term water balance changes in lakes of different statuses. The main findings, hypotheses, and contributions for each of the objectives mentioned are discussed below.

Chapter two covers the first objective of this study, to identify changes occurring in endorheic basins by comparing Lake Turkana to the Aral Sea. In this chapter, the changes that transpired in the Aral Sea basin were described to highlight the expected changes in the Lake Turkana basin. The primary data source used here is the literature review of multiple studies. Here, the expansion of the irrigated area in the Aral Sea basin was reported to have resulted in excessive water use.

This growth, in turn, propagated increased secondary soil salinization. By 1994, with approximately 79000km^2 of irrigated area, 40 percent of irrigated land in Central Asia was classified as saline. Additionally, an inverse trend was established between the growing irrigated area and the reduction in Sea area. When a 13 percent increase in the irrigated area occurred from 1960 to 1970, a 10 percent drop in sea level was experienced.

Moreover, a similar inverse trend was described between the increase in salinity and reducing fishing stocks. When the salinity levels in the Sea got to approximately 22 grams per liter, the total collapse of the fishing industry occurred. At this level, only salt-tolerant fish could survive in the Sea. Finally, a reduction in the Sea level resulted in increased disease incidents in the Aral Sea basin. In the 1970s and 1980s, the Sea area had decreased by nearly half. During this period, it was reported that approximately 60 percent of children under the age of one who died in the Karakalpakstan region died of respiratory diseases.

In chapter 4, objectives 2 and 3 are covered. Three indices were developed to improve the detection of irrigation areas using the land surface model's analyzed radiative temperature and satellite-based land surface temperature. The results show the ability of these indices to detect the irrigation effect even in drought years. A sum of each index compared to water availability provided by dam data also showed a similar trend, indicating the indices' ability to capture changes in the irrigated area. Additionally, Remote sensing for the detection of salinity in this basin indicated the limitation instigated by the coarse satellite resolution. No significant correlation was established between the indices employed and salinity in the basin. However, the reflectance-based indices generally exhibited an increasing trend with an increase in salinity, while the vegetation indices decreased with an increase in salinity. Since the effects of soil salinization are mainly localized, a basin-scale analysis may be too coarse for the effective detection of salinity. Additionally, at the satellite’s resolution, farmlands

with many different crop types may be represented by a single pixel. This representation will lead to the mixed-cell effect where the retrieved reflectance data is contaminated by the influence of different crop types and varying crop health.

In chapter 5, An endorheic lake water balance model was developed to estimate changes in the water circulation in the basin. This model was able to replicate trends in the changing water balance from 2001 to 2018. This trend showed a relatively strong correlation with a Pearson's coefficient (r) of 0.82. The changing climate, particularly precipitation, was established to be the main driver for storage changes in this basin.

Finally, in Chapter 6, the sustainability of endorheic lakes is evaluated against the variability in area and volume. It is elucidated that examining the variation of both volume and area in an endorheic lake can provide some insight into the lake's status. The larger the changes in the trend, the more significant the impact of changes in water balance on the surrounding environment. Furthermore, examining changes in both area and volume variation can provide insight into the magnitude of short-term changes in the lake.

7.2 Recommendations for further studies

In detecting the irrigated area using LST indices, the analysis involved the summation of indices only. However, these results may be affected by meshes with extreme value. For further research, the irrigation fraction of all meshes need to be analyzed more precisely and verified by local data.

Since the effects of soil salinization are mainly localized, a basin-scale analysis may be too coarse for the effective detection of salinity. Additionally, at the satellite's resolution, farmlands with many different crop types may be represented by a single pixel. This representation will lead to the mixed-cell effect where the retrieved reflectance data is

contaminated by the influence of different crop types and varying crop health. Therefore, a higher resolution remote sensing technique is required for effective salinity detection

References

ADB, 2010. Central Asia ATLAS of Natural Resources. Central Asian Countries Initiative for Land Management Asian Development Bank Manila, Philippines. ADB Manila, Philippines, Manila, Philippines.

Adrian, R., O'Reilly, C.M., Zagarese, H., Baines, S.B., Hessen, D.O., Keller, W., Livingstone, D.M., Sommaruga, R., Straile, D., Van Donk, E., Weyhenmeyer, G.A., Winder, M., 2009. Lakes as sentinels of climate change. Limnol. Oceanogr. 54, 2283–2297. https://doi.org/10.4319/lo.2009.54.6_part_2.2283

Arino, O., Arino, O., Gross, D., Gross, D., Ranera, F., Ranera, F., 2000. GlobCover: ESA service for Global Land Cover from MERIS. Processing 2412–2415.

Avery, S., 2014. What future for Lake Turkana and its wildlife. SWARA (Magazine East African Wildl. Soc.

Avery, S., 2012a. Lake Turkana & The Lower Omo: Hydrological Impacts of Major Dam & Irrigation Developments Volume II - Annexes.

Avery, S., 2012b. Lake Turkana & The Lower Omo: Hydrological Impacts of Major Dam & Irrigation Developments Volume I - Report.

Avery, S., 2010. Hydrological Impacts Of Ethiopia's Omo Basin On Kenya's Lake Turkana Water Levels & Fisheries Final Report.

Avery, S.T., Tebbs, E.J., 2018a. Lake Turkana, major Omo River developments, associated hydrological cycle change and consequent lake physical and ecological change. J. Great Lakes Res. 44, 1164–1182. https://doi.org/10.1016/j.jglr.2018.08.014

Avery, S.T., Tebbs, E.J., 2018b. Lake Turkana, major Omo River developments, associated hydrological cycle change and consequent lake physical and ecological change. J. Great Lakes Res. 44, 1164–1182. https://doi.org/10.1016/j.jglr.2018.08.014

Awulachew, S.B., Yilma, A.D., Loulseged, M., Loiskandl, W., Ayana, M., Alamirew, T., 2007. Water Resources and Irrigation Development in Ethiopia (No. 123). Colombo, Sri Lanka.

Bai, J., Chen, X., Li, J., Yang, L., Fang, H., 2011. Changes in the area of inland lakes in arid regions of central Asia during the past 30 years. Environ. Monit. Assess. 178, 247–256. https://doi.org/10.1007/s10661-010-1686-y

Bekchanov, M., Ringler, C., Bhaduri, A., Jeuland, M., 2016. Optimizing irrigation efficiency improvements in the Aral Sea Basin. Water Resour. Econ. 13, 30–45. https://doi.org/10.1016/j.wre.2015.08.003

Birkett, C.M., 2000. Synergistic remote sensing of Lake Chad: Variability of basin inundation. Remote Sens. Environ. 72, 218–236. https://doi.org/10.1016/S0034-4257(99)00105-4

Boretti, A., Rosa, L., 2019. Reassessing the projections of the World Water Development Report. npj Clean Water 2. https://doi.org/10.1038/s41545-019-0039-9

Bouaziz, M., Matschullat, J., Gloaguen, R., 2011. Improved remote sensing detection of soil salinity from a semi-arid climate in Northeast Brazil. Comptes Rendus - Geosci. 343, 795–803. https://doi.org/10.1016/j.crte.2011.09.003

Bruinsma, J., 2017. World agriculture: Towards 2015/2030: An FAO Study. World Agric. Towar. 2015/2030 An FAO Study 1–431. https://doi.org/10.4324/9781315083858

Bucknall, J., Klytchnikova, I., Lampietti, J., Lundell, M., Scatasta, M., Thurman, M., 2003. Irrigation in Central Asia. Social, economic and environmental considerations. Eur. Cent. Asia Reg. 104.

Butzer, K.W., 1970. Contemporary Depositional Environments of the Omo Delta. Nature 266, 425–430. https://doi.org/doi:10.1038/226425a0

CA Water, 2005. Physical-geographic characteristics of the region. CA Water Info. URL http://www.cawater-info.net/bk/water_land_resources_use/english/docs/fiziko_geog_kharack_regiona.html

Carr, C.J., 2017. River Basin Development and Human Rights in Eastern Africa - A Policy Crossroads, River Basin Development and Human Rights in Eastern Africa - A Policy Crossroads. https://doi.org/10.1007/978-3-319-50469-8

CAWaterinfo, 2005a. CAWaterinfo. Aral Sea. URL http://www.cawater-info.net/aral/geo_e.htm (accessed 7.18.18).

CAWaterinfo, 2005b. CAWaterinfo. Aral Sea.

CCPO-ODU, 2015. Center for Coastal Physical Oceanography. Studying Earths Environment from Space. Chapter 4: Plant and Vegetation Community Properties. URL http://www.ccpo.odu.edu/SEES/veget/class/Chap_4/4_ref.htm (accessed 7.12.18).

Chen, D.-H., 2018. Once Written Off for Dead, the Aral Sea Is Now Full of Life. Natl. Geogr. Mag.

Clack, T., 2018. ‘World’s worst environmental disaster’ set to be repeated with controversial new dam in Africa. Conversat. URL https://theconversation.com/worlds-worst-environmental-disaster-set-to-be-repeated-with-controversial-new-dam-in-africa-107070

Conrad, C., Dech, S.W., Hafeez, M., Lamers, J., Martius, C., Strunz, G., 2007. Mapping and assessing water use in a Central Asian irrigation system by utilizing MODIS

remote sensing products. Irrig. Drain. Syst. 21, 197–218. https://doi.org/10.1007/s10795-007-9029-z

Copertino, V.A., Di Pierro, M., Scavone, G., Telesca, V., 2012. Comparison of algorithms to retrieve land surface temperature from LANDSAT-7 ETM+ IR data in the basilicata ionian band. Tethys 2012, 25–34. https://doi.org/10.3369/tethys.2012.9.03

Derbyshire, S.F., 2019. Trade, development and destitution: A material culture history of fishing on the western shore of Lake Turkana, northern Kenya. Afr. Stud. 78, 324–346. https://doi.org/10.1080/00020184.2018.1519930

Dowgert, M., 2010. The Impact of Irrigated Agriculture on a Stable Food Supply. Proc. 22nd Annu. Cent. Plains Irrig. Conf. 1–11.

Droogers, P., 2002. Global irrigated area mapping: Overview and recommendations. Colombo, Sri Lanka.

Elhag, M., 2016. Evaluation of Different Soil Salinity Mapping Using Remote Sensing Techniques in Arid Ecosystems, Saudi Arabia. J. Sensors 2016. https://doi.org/10.1155/2016/7596175

Eurasianet, 2016. Uzbekistan's Losing Battle Against Drought. URL https://eurasianet.org/uzbekistans-losing-battle-against-drought (accessed 5.29.19).

FAO, 2016a. AQUASTAT website. Food and Agriculture Organization of the United Nations. URL http://www.fao.org/nr/water/aquastat/countries_regions/profile_segments/aral.sea-IrrDr_eng.stm (accessed 7.11.18).

FAO, 2016b. AQUASTAT Country profile – Ethiopia 1–21.

FAO, 2016c. AQUASTAT website. Food and Agriculture Organization. Central asia. URL http://www.fao.org/nr/water/aquastat/countries_regions/profile_segments/asiaC-EnvHea_eng.stm (accessed 5.27.19).

FAO, 2012. AQUASTAT Transboundary River Basin Overview – Aral Sea, FAO Aquastat Reports. Rome, Italy.

FAO, 1988. FAO/UNESCO Soil Map of the World: World Soil Resources Report 60.

Farr, T.G., Kobrick, M., 2000. Defense Technical Information Center Compilation Part Notice TITLE : The Shuttle Radar Topography Mission.

Frenken, K., 2005. Irrigation in Africa in figures: AQUASTAT survey, Food and Agricultural Organisation.

Frenken, K. (FAO), 2012. Irrigation in Central Asia in figures. AQUASTAT Survey-2012, Irrigation in Central Asia in figures. AQUASTAT Survey-2012.

Glantz, M.H., 1999. Creeping environmental problems and sustainable development in the Aral Sea basin. Cambridge University Press.

Gleick, P.H., 2000. A Look at Twenty-first Century Water Resources Development. Water Int. 25, 127–138. https://doi.org/10.1080/02508060008686804

Government of Ethiopia, 2018. State party report on the state of conservation of Lower Valley of the Omo. Ethiopia.

Guganesharajah, K., Shaw, E.M., 1984. Forecasting Water Levels for Lake Chad. Water Resour. Res. 20, 1053–1065. https://doi.org/10.1029/WR020i008p01053

Gumma, M.K., Thenkabail, P.S., Maunahan, A., Islam, S., Nelson, A., 2014. Mapping seasonal rice cropland extent and area in the high cropping intensity environment of Bangladesh using MODIS 500m data for the year 2010. ISPRS J. Photogramm. Remote Sens. 91, 98–113. https://doi.org/10.1016/j.isprsjprs.2014.02.007

Hausfather, Z., 2019. CMIP6: the next generation of climate models explained. CarbonBrief.

Herrmann, S.M., Mohr, K.I., 2011. A continental-scale classification of rainfall seasonality regimes in Africa based on gridded precipitation and land surface temperature products. J. Appl. Meteorol. Climatol. 50, 2504–2513. https://doi.org/10.1175/JAMC-D-11-024.1

Hirabayashi, Y., Kanae, S., Emori, S., Oki, T., Kimoto, M., 2008. Global projections of changing risks of floods and droughts in a changing climate. Hydrol. Sci. J. 53, 754–772. https://doi.org/10.1623/hysj.53.4.754

Hodbod, J., Stevenson, E.G.J., Akall, G., Akuja, T., Angelei, I., Bedasso, E.A., Buffavand, L., Derbyshire, S., Eulenberger, I., Gownaris, N., Kamski, B., Kurewa, A., Lokuruka, M., Mulugeta, M.F., Okenwa, D., Rodgers, C., Tebbs, E., 2019. Social-ecological change in the Omo-Turkana basin: A synthesis of current developments. Ambio 48, 1099–1115. https://doi.org/10.1007/s13280-018-1139-3

Hopson, A.J., 1982. Lake Turkana: a report on thefindings of the Lake Turkana project 1972–1975.

Ibrakhimov, M., Khamzina, A., Forkutsa, I., Paluasheva, G., Lamers, J.P.A., Tischbein, B., Vlek, P.L.G., Martius, C., 2007. Groundwater table and salinity: Spatial and temporal distribution and influence on soil salinization in Khorezm region (Uzbekistan, Aral Sea Basin). Irrig. Drain. Syst. 21, 219–236. https://doi.org/10.1007/s10795-007-9033-3

IFAS–UNEP, 2001. International Fund for the Aral Sea and the UN Environment Programme. Environment State of the Aral Sea Basin — Regional Report of the Central Asian States 2000.

IPCC, 2014. Summary for policymakers. In Climate change 2014: impacts, adaptation, and vulnerability. Part A: global and sectoral aspects. Contribution of Working Group II to the Fifth Assessment Report of the Intergovernmental Panel on Climate Change. Cambridge University Press, Cambridge, United Kingdom and New York,NY, USA. https://doi.org/10.1136/bmj.g5945

Irmak, S., Odhiambo, L.O., Kranz, W.L., Eisenhauer, D.E., 2011. Irrigation Efficiency and Uniformity, and Crop Water Use Efficiency. Biol. Syst. Eng. Pap. Publ. 451. https://doi.org/10.13031/trans.59.11331

IUCN, 2020. Lake Turkana Natural Parks 2020 Conservation Outlook Assessment 2020 Conservation Outlook.

JICA, 2012. Water Potential Study in Turkana County.

Johnson, T.C., Malala, J.O., 2009. Lake Turkana and its link to the Nile., in: Dumont, H.J. (Ed.), The Nile: Origin, Environments, Limnology and Human Use. Springer Science & Business Media, pp. 297–304.

Jury, M.R., 2011. Meteorological scenario of Ethiopian floods in 2006-2007. Theor. Appl. Climatol. 104, 209–219. https://doi.org/10.1007/s00704-010-0337-0

Kaijage, A.S., Nyagah, N.M., 2009. Socio-economic analysis and public consultation of Lake Turkana communities in northern Kenya.

Kamski, B., 2016. The Kuraz Sugar Development Project (KSDP) in Ethiopia: between 'sweet visions' and mounting challenges. J. East. African Stud. 10, 568–580. https://doi.org/10.1080/17531055.2016.1267602

Khan, N.M., Rastoskuev, V. V., Sato, Y., Shiozawa, S., 2005. Assessment of hydrosaline land degradation by using a simple approach of remote sensing indicators. Agric. Water Manag. 77, 96–109. https://doi.org/10.1016/j.agwat.2004.09.038

Khujanazarov, T., Ichikawa, Y., Abdullaev, I., Toderich, K., 2012. Water Quality Monitoring and Geospatial Database Coupled with Hydrological Data of Zeravshan River Basin 202, 199–202.

KNBS, 2019. 2019 Kenya Population and Housing Census Volume 1: Population by County and Sub-County, 2019 Kenya Population and Housing Census.

Kobayashi, S., Ota, Y., Harada, Y., Ayataka, E., Moriya, M., Onoda, H., Onogi, K., Kamahori, H., Kobayashi, C., Endo, H., Miyaoka, K., Takahashi, K., 2015. The JRA-55 Reanalysis: General Specifications and Basic Characteristics. J. Meteorol. Soc. Japan. Ser. II 93, 5–48. https://doi.org/10.2151/jmsj.2015-001

Li, B., Li, J., Chen, J., Yu, J., 2009. Saline Lakes Around the World: Unique Systems with Unique Values Article. Nat. Resour. Environ. Issues 15, 43.

Li, X., Troy, T.J., 2018. Changes in rainfed and irrigated crop yield response to climate in the western US. Environ. Res. Lett. 13. https://doi.org/10.1088/1748-9326/aac4b1

Lobell, D.B., Lesch, S.M., Corwin, D.L., Ulmer, M.G., Anderson, K.A., Potts, D.J., Doolittle, J.A., Matos, M.R., Baltes, M.J., 2010. Regional-scale Assessment of Soil Salinity in the Red River Valley Using Multi-year MODIS EVI and NDVI. J. Environ. Qual. 39, 35. https://doi.org/10.2134/jeq2009.0140

Loveland, T.R., Reed, B.C., Brown, J.F., Ohlen, D.O., Zhu, Z., Yang, L., Merchant, J.W., 2000. Development of a global land cover characteristics database and IGBP DISCover from 1 km AVHRR data. Int. J. Remote Sens. 21, 1303–1330. https://doi.org/10.1080/014311600210191

Luo, W., Gao, X., Zhang, X., 2018. Geochemical processes controlling the groundwater chemistry and fluoride contamination in the yuncheng basin, China—an area with complex hydrogeochemical conditions. PLoS One 13, 1–25. https://doi.org/10.1371/journal.pone.0199082

Luttah, S., 2020. Kenya: Fears of Cholera, Kala-Azar Outbreaks as Lake Turkana Continues to Swell. Dly. Nation.

Maina, B.M., Ragwa, P.K., Wahome, R.G., Karanja, R., Mwathe, H., Ndirangu, G.M., Kinya, J., Muriuki, M., Muthoni, P., 2013. OPPORTUNITIES AND THREATS OF IRRIGATION DEVELOPMENT IN KENYA ' S DRYLANDS Volume VI : Turkana County VI.

Malala, J., Olilo, C., Keyombe, J., Obiero, M., Bironga, C., Aura, C., Wakwabi, E., Njiru, J., 2018. Catch Assessment Survey (CAS) report for Lake Turkana and to disseminate the findings.

Masson, V., Champeaux, J.L., Chauvin, F., Meriguet, C., Lacaze, R., 2003. A global database of land surface parameters at 1-km resolution in meteorological and climate models. J. Clim. 16, 1261–1282. https://doi.org/10.1175/1520-0442-16.9.1261

Mbugua, J.M., 2018. Remotely Sensed Spatial and Temporal Variability of Drought and Salinization in Irrigated Area in the Aral Sea Basin. Tohoku University.

Metternicht, G.I., Zinck, J.A., 2003. Remote sensing of soil salinity: Potentials and constraints. Remote Sens. Environ. 85, 1–20. https://doi.org/10.1016/S0034-4257(02)00188-8

Micklin, P., 2010. The past, present, and future Aral Sea. Lakes Reserv. Res. Manag. 15, 193–213. https://doi.org/10.1111/j.1440-1770.2010.00437.x

Micklin, P., 2000. Managing Water in Central Asia. Royal Institute of International Affairs.

Micklin, P., Aladin, N. V., Plotnikov, I.S., 2014. The aral sea: The devastation and partial rehabilitation of a great lake, The Aral Sea: The Devastation and Partial Rehabilitation of a Great Lake. https://doi.org/10.1007/978-3-642-02356-9

Micklin, P., Aladin, N. V, 2008. Reclaiming the Aral Sea. Sci. Am. 298, 64–71. https://doi.org/10.1038/scientificamerican0408-64

Molden, B. and D.J., 2000. Remote sensing for irrigated agriculture : examples from research and possible applications . Agric . Water Manag Remote sensing for irrigated agriculture : examples from research and possible applications. Agric. Water Manag. 46, 137–155. https://doi.org/10.1016/S0378-3774(00)00080-9

Mottaleb, K.A., Krupnik, T.J., Keil, A., Erenstein, O., 2019. Understanding clients, providers and the institutional dimensions of irrigation services in developing countries: A study of water markets in Bangladesh. Agric. Water Manag. 222, 242–253. https://doi.org/10.1016/j.agwat.2019.05.038

Mwikya, S.M., 2005. Lake Turkana Fishery : Options for Development of a Sustainable Trade.

Nazirov, A.A., 2005. Central Asia: Water for Food (No. 31).

Nicholson, S.E., 2014. A detailed look at the recent drought situation in the Greater Horn of Africa. J. Arid Environ. 103, 71–79. https://doi.org/10.1016/j.jaridenv.2013.12.003

Nur, M., Vella, J.P., Ses, S., 2003. Gridding Digitized Bathymetry in the Straits of Malacca. Ceoinformation Sci. J. 3, 24–28.

Obiero, K., Donde, O., Gownaris, N., Pikitch, E.K., 2016. The Wetland Book. Wetl. B. https://doi.org/10.1007/978-94-007-6173-5

OCHA, 2011. Eastern Africa Drought Humanitarian Report No. 3.

Olaka, L.A., Odada, E.O., Trauth, M.H., Olago, D.O., 2010. The sensitivity of East African rift lakes to climate fluctuations. J. Paleolimnol. 44, 629–644. https://doi.org/10.1007/s10933-010-9442-4

Ondimu, K.. I., Chemoiwo, M., Kemboi, J., 2018. Blue Economy Bankable Projects.

Orlovsky, N., Orlovsky, L., Yang, Y., Xiao, H., 2003. Salt duststorms of Central Asia since 1960s. J. Desert Res. 18–27.

OTuRN, 2017. Change in the Omo-Turkana Basin. URL https://www.canr.msu.edu/oturn/change-in-the-omo-turkana-basin

Owens, S., 2001. Tackling the most difficult diseases. Genetics and genomics open new strategies to fight vector-borne diseases. EMBO Rep. 2, 875–877. https://doi.org/10.1093/embo-reports/kve218

Passey, B.H., Levin, N.E., Cerling, T.E., Brown, F.H., Eiler, J.M., 2010. High-temperature environments of human evolution in East Africa based on bond ordering in paleosol carbonates. Proc. Natl. Acad. Sci. U. S. A. 107, 11245–11249. https://doi.org/10.1073/pnas.1001824107

Peachey, E.J., 2004. the Aral Sea Basin Crisis and Sustainable Water Resource Management in Central Asia. J. Public Int. Aff. 15, 1–20.

Petr, T., Ismukhanov, K., Kamilov, B., Pulakhton, D., Umarov, P., 2004. Irrigation systems and their fisheries in the Aral Sea Basin, central Asia. Proc. Second Int. Symp. Manag. Large Rivers Fish. 2, 223–242.

Pingali, P. L. & Heisey, P.W., 1999. Cereal crop productivity in developing countries. CIMMYT Econ. Pap. CIMMYT, Mex. DF. 99–03.

Qiu, R., Liu, C., Wang, Z., Yang, Z., Jing, Y., 2017. Effects of irrigation water salinity on evapotranspiration modified by leaching fractions in hot pepper plants. Sci. Rep. 7, 1–11. https://doi.org/10.1038/s41598-017-07743-2

Ricketts, R.D., Johnson, T.C., 1996. Climate change in the Turkana basin as deduced from a 4000 year long δO18 record. Earth Planet. Sci. Lett. 142, 7–17. https://doi.org/10.1016/0012-821x(96)00094-5

Ringler, C., 2012. Water use and economic growth in the anthropocene. Glob. water news. URL https://water-future.org/gwsp-archive-water-econgrowth/

Rodionov, S., 2012. Global and regional climate interaction: the Caspian Sea experience. Springer Sci. Bus. Media 11.

Rosegrant, M., Cai, X., Cline, S., Nakagawa, N., 2002. The Role of Rainfed Agriculture in the Future of Global Food Production. Environ. Prod. Technol. Div. 127.

Ryan, J., Vlek, P., Paroda, R., 2004. Agriculture in Central Asia: Research for development. ICARDA.

Salini Impregilo, 2019. Gibe III Hydroelectric Project. Webuild. URL https://www.webuildgroup.com/en/projects/dams-hydroelectric-plants/gibe-iii-hydroelectric-project

Salini Impregilo, 2016. Ethiopia inaugurates tallest RCC dam in world built by Webuild. Webuild. URL https://www.webuildgroup.com/en/media/press-releases/ethiopia-inaugurates-tallest-rcc-dam-in-world-built-by-salini-impregilo

Sehler, R., Li, J., Reager, J., Ye, H., 2019. Investigating Relationship Between Soil Moisture and Precipitation Globally Using Remote Sensing Observations. J. Contemp. Water Res. Educ. 168, 106–118. https://doi.org/10.1111/j.1936-704x.2019.03324.x

Sellers, P.., Mintz, Y.C.S.., Sud, Y.E.., Dalcher, A., 1986. A simple biosphere model (SiB) for use within general circulation models. J. Atmos. Sci. 43, 505–531.

Senay, G.B., 2008. Modeling landscape evapotranspiration by integrating land surface phenology and a water balance algorithm. Algorithms 1, 52–68. https://doi.org/10.3390/a1020052

Shiklomanov, I.A., 2000. Appraisal and Assessment of world water resources. Water Int. 25, 11–32. https://doi.org/10.1080/02508060008686794

Siebert, S., Döll, P., Hoogeveen, J., Faures, J.M., Frenken, K., Feick, S., 2005. Development and validation of the global map of irrigation areas. Hydrol. Earth Syst. Sci. 9, 535–547. https://doi.org/10.5194/hess-9-535-2005

Sindhu, B., Suresh, I., Unnikrishnan, A.S., Bhatkar, N. V., Neetu, S., Michael, G.S., 2007. Improved bathymetric datasets for the shallow water regions in the Indian Ocean. J. Earth Syst. Sci. 116, 261–274. https://doi.org/10.1007/s12040-007-0025-3

SOGREAH, 2010. Independent review and studies regarding the environmental and social impact assessments for the Gibe 3 hydrolectric project.

Spruill, J., 2019. Assessing Hydrological Impacts Of The Gilgel Gibe Iii Dam On Lake Turkana Water Levels. Johns Hopkins University.

Tanaka, K., 2005. Development of the new land surface scheme SiBUC commonly applicable to basin water management and numerical weather prediction model. PhD thesis. Kyoto University.

The Oakland Institute, 2019. “How They Tricked Us” - Living with the Gibe III Dam and Sugarcane Plantations in Southwest Ethiopia 22.

The World Bank, 2019a. Population, total - Kazakhstan, Kyrgyz Republic, Tajikistan, Turkmenistan, Uzbekistan. World Bank Data. URL https://data.worldbank.org/indicator/SP.POP.TOTL?locations=KZ-KG-TJ-TM-UZ

The World Bank, 2019b. Population growth (annual %) - Ethiopia | Data. World Dev. Indic. URL https://data.worldbank.org/indicator/SP.POP.GROW?locations=ET

The World Bank, 2017. Annual freshwater withdrawals, total (billion cubic meters) - Kazakhstan, Kyrgyz Republic, Tajikistan, Turkmenistan, Uzbekistan. World bank data. URL https://data.worldbank.org/indicator/ER.H2O.FWTL.K3?contextual=similar&end=2017&locations=KZ-KG-TJ-TM-UZ&start=2017&view=bar

Toderich, K., Ismail, S., Massino, I., Wilhelm, M., Yusupov, S., Kuliev, T., 2008. Extent of salt-affected land in Central Asia: Biosaline agriculture and utilization of the salt-affected resources, Advances in assessment and monitoring of salinization and status of biosaline agriculture. Reports of expert consultation, Dubai, UAE. World Soil Resources Reports No. 104.

Touge, Y., Tanaka, K., Kojiri, T., Hamaguchi, T., 2013. Reproducing Shrinking of the Aral Sea by Analyzing Water and Heat Balances Considering the Impacts of Expanding Irrigated Area. Environ. Sci. 26, 180–190. https://doi.org/10.11353/sesj.26.180

Touge, Y., Tanaka, K., Nakakita, E., 2015. Estimation of Climate Change Impacts on Water Balance in the Aral Sea Basin using Terrestrial Water Circulation Model. J. Japan Soc. Civ. Eng. Ser. G (Environmental Res. 71, I_183-I_188.

Turkana County Government, 2015. Turkana County Annual Development Plan.

UNEP, 2013. Ethiopia's Gibe III Dam: its Potential Impact on Lake Turkana Water Levels (A case study using hydrologic modelling and multi-source satellite data).

UNESCO, 2020. Lake Turkana National Parks. World Herit. Outlook. URL https://worldheritageoutlook.iucn.org/explore-sites/wdpaid/145586

UNESCO, 2018. The United Nations world water development report 2018: Nature-Based Solutions for Water, Unesco.

UNESCO, 2012. Water in a changing world the United Nations world water development report 3, The United Nations World Water Development Report 3: Water in a Changing World (Two Vols.).

United Nations, 2017. World Population Prospects: The 2017 Revision, Key Findings and Advance Tables.

USDA, 2016. Global Reservoirs and Lakes Monitor (G-REALM). URL https://ipad.fas.usda.gov/cropexplorer/global_reservoir/

Ushio, T., Sasashige, K., Kubota, T., Shige, S., Okamoto, K., Aonashi, K., Inoue, T., Takahashi, N., Iguchi, T., Kachi, M., Oki, R., Morimoto, T., Kawasaki, Z.I., 2009. A kalman filter approach to the global satellite mapping of precipitation (GSMaP) from combined passive microwave and infrared radiometric data. J. Meteorol. Soc. Japan 87 A, 137–151. https://doi.org/10.2151/jmsj.87A.137

Velpuri, N.M., Senay, G.B., Asante, K.O., 2012. A multi-source satellite data approach for modelling Lake Turkana water level: Calibration and validation using satellite altimetry data. Hydrol. Earth Syst. Sci. 16, 1–18. https://doi.org/10.5194/hess-16-1-2012

Verburg, P., Hecky, R.E., Kling, H., 2003. Ecological Consequences of a Century of Warming in Lake Tanganyika. Science (80-.). 301, 2002–2004.

Vermote, E.., Kotchenova, S.., Ray, J.., 2011. MODIS Surface Reflectance User ' s Guide. Orbit An Int. J. Orbital Disord. Facial Reconstr. Surg. 1–40.

Vörösmarty, C.J., 2002. Global water assessment and potential contributions from Earth Systems Science. Aquat. Sci. 64, 328–351. https://doi.org/10.1007/PL00012590

Wada, Y., Flörke, M., Hanasaki, N., Eisner, S., Fischer, G., Tramberend, S., Satoh, Y., Van Vliet, M.T.H., Yillia, P., Ringler, C., Burek, P., Wiberg, D., 2016. Modeling global water use for the 21st century: The Water Futures and Solutions (WFaS) initiative and

its approaches. Geosci. Model Dev. 9, 175–222. https://doi.org/10.5194/gmd-9-175-2016

Wan, Z., Hook, S., Hulley, G., 2015. MODIS Land Surface Temperature Products Users ' Guide. Qual. Assur. 35. https://doi.org/10.5067/MODIS/MOD11B3.006

Wan, Z., Wang, P., Li, X., 2004. Using MODIS Land Surface Temperature and Normalized Difference Vegetation Index products for monitoring drought in the southern Great Plains, USA. Int. J. Remote Sens. 25, 61–72. https://doi.org/10.1080/0143116031000115328

Wang, D., Poss, J.A., Donovan, T.J., Shannon, M.C., Lesch, S.M., 2002. Biophysical properties and biomass production of elephant grass under saline conditions. J. Arid Environ. 52, 447–456. https://doi.org/10.1006/jare.2002.1016

Wardlow, B.D., Egbert, S.L., Kastens, J.H., 2007. Analysis of time-series MODIS 250 m vegetation index data for crop classification in the U.S. Central Great Plains. Remote Sens. Environ. 108, 290–310. https://doi.org/10.1016/j.rse.2006.11.021

Water FAO, 2009. Water at a Glance. The relationship between water, agriculture, food security and poverty. Rome.

Wiegand, C.L., Rhoades, J.D., Escobar, D.E., Everitt, J.H., 1994. Photographic and videographic observations for determining and mapping the response of cotton to soil salinity. Remote Sens. Environ. 49, 212–223. https://doi.org/10.1016/0034-4257(94)90017-5

Woldegebrael, S.M., Kidanewold, B.B., Zaitchik, B., Melesse, A.M., 2020. Rainfall and Flood Event Interrelationship - A Case Study of Awash and Omo-Gibe Basins, Ethiopia. Int. J. Sci. Eng. Res. 11.

Worldometer, 2021. Central Asia Population. URL https://www.worldometers.info/world-population/central-asia-population/#:~:text=Countries in Central Asia&text=The population density in Central,49 people per mi2).

Yamazaki, D., Ikeshima, D., Sosa, J., Bates, P.D., Allen, G.H., Pavelsky, T.M., 2019. MERIT Hydro: A High-Resolution Global Hydrography Map Based on Latest Topography Dataset. Water Resour. Res. 55, 5053–5073. https://doi.org/10.1029/2019WR024873

Zheng, H., Ying, H., Yin, Y., Wang, Y., He, G., Bian, Q., Cui, Z., Yang, Q., 2019. Irrigation leads to greater maize yield at higher water productivity and lower environmental costs: a global meta-analysis. Agric. Ecosyst. Environ. 273, 62–69. https://doi.org/10.1016/j.agee.2018.12.009

ZOï maps, 2016. ZOï Environmental Network. Zeravshan River Basin. URL https://www.flickr.com/photos/zoienvironment/38646123642/in/photostream/# (accessed 7.15.18).